INFORMATION TO USERS

This manuscript has been reproduced from the microfilm master. UMI films the text directly from the original or copy submitted. Thus, some thesis and dissertation copies are in typewriter face, while others may be from any type of computer printer.

The quality of this reproduction is dependent upon the quality of the copy submitted. Broken or indistinct print, colored or poor quality illustrations and photographs, print bleedthrough, substandard margins, and improper alignment can adversely affect reproduction.

In the unlikely event that the author did not send UMI a complete manuscript and there are missing pages, these will be noted. Also, if unauthorized copyright material had to be removed, a note will indicate the deletion.

Oversize materials (e.g., maps, drawings, charts) are reproduced by sectioning the original, beginning at the upper left-hand corner and continuing from left to right in equal sections with small overlaps.

ProQuest Information and Learning
300 North Zeeb Road, Ann Arbor, MI 48106-1346 USA
800-521-0600

UMI®

HYDRODENITROGENATION OF PYRIDINE

OVER

COBALT-MOLYBDATE CATALYST

by

RAJNISH KUMAR GUPTA

A thesis submitted to the School of Graduate Studies
in partial fulfillment of the requirements for the
degree of

MASTER OF APPLIED SCIENCE

in the

DEPARTMENT OF CHEMICAL ENGINEERING

UNIVERSITY OF OTTAWA

Ottawa, Canada

July 1977

Research Director

M.A.Sc. Candidate

© R.K. Gupta, Ottawa, Canada, 1977

UMI Number: EC52247

INFORMATION TO USERS

The quality of this reproduction is dependent upon the quality of the copy submitted. Broken or indistinct print, colored or poor quality illustrations and photographs, print bleed-through, substandard margins, and improper alignment can adversely affect reproduction.

In the unlikely event that the author did not send a complete manuscript and there are missing pages, these will be noted. Also, if unauthorized copyright material had to be removed, a note will indicate the deletion.

UMI®

UMI Microform EC52247
Copyright 2007 by ProQuest LLC
All rights reserved. This microform edition is protected against unauthorized copying under Title 17, United States Code.

ProQuest LLC
789 East Eisenhower Parkway
P.O. Box 1346
Ann Arbor, MI 48106-1346

ACKNOWLEDGEMENT

The author would like to express his sincere thanks and gratitude to his Research Director, Prof. R.S. Mann for his patience, guidance and encouragement throughout the course of this project and his help in the preparation of this thesis.

Thanks are due to Mr. G. Gasperetti for the installation and maintenance of the apparatus; Mr. N. Tan for his numerous suggestions; Dr. A. Shah for his proof reading and Mrs. S. Ryan for typing the manuscript.

Finally, the author is indebted to the Department of Energy, Mines, and Resources for financial aid for this project (2239-2-12-7-77).

TABLE OF CONTENTS

LIST OF FIGURES

ABSTRACT

The vapour phase hydrogenation of pyridine was investigated in an integral flow reactor at a pressure of 5.617 M Pa over alumina-supported cobalt-molybdate catalyst.

The effect of various process variables viz. temperature, reactant ratio and space time on the conversion of pyridine was studied. The kinetics of the hydrogenation of pyridine to form piperidine have been investigated.

The reaction showed zero-order kinetics. However, the zero-order reaction rate constant, K, was found to be a function of the initial pyridine concentration, C_{p_o} :

$$K = K_p \, (C_{p_o})^n$$

where n is the order of the reaction rate constant in C_{p_o}

and K_p is a pseudo-rate constant.

The order, n, was found to vary with temperature and could be expressed as:

$$\ell n \; n = 33.05 - 5.40 \; \ell n \; T$$

$$(388°K < T < 433°K)$$

where T is the absolute temperature, °K.

The pseudo-second-order rate constant, K_p (for n=2), could be expressed as:

$$\ell n \; K_p = 17.025 - \frac{11514}{RT}$$

where R is the universal gas constant, cal-gmole^{-1}-°K^{-1}.

CHAPTER 1

INTRODUCTION

Pyridine, along with quinoline, is one of the model nitrogen-bearing compounds whose derivatives occur in crude oil and coal. These compounds cause severe corrosion and catalyst-poisoning in the storage and processing of crude oils in the refining process. Their presence in finished petroleum products is also undesirable because of the formation of nitrogen oxides upon combustion in engines and because of their effect on the viscosity of lube oils. As such, it would be highly desirable to remove these compounds in the initial stages of the refining process. Hydrodenitrogenation (HDN) seems to be the most viable method of achieving this.

The HDN of pyridines and quinolines has not gained industrial significance yet because of the rather low nitrogen content of premium grades of crude oil whose reserves, until a few years ago, seemed to be inexhaustible. However, with the depletion of these reserves, progressively lower grades of crude oil (containing larger amounts of nitrogen compounds) and synthetic crude oil (also having a very high nitrogen content) made from coal and oil-shale will have to be used. It is therefore expected that in a few years, the HDN reaction will be of paramount importance. For this reason, a study of the HDN reaction was undertaken.

Pyridine was chosen as the model compound because a large percentage of the nitrogen-bearing compounds present in crude oil are derivatives of pyridine. The kinetics and mechanism of this reaction are not as yet fully understood in spite of a number of studies in this

field[1-10].

The catalyst chosen - cobalt-molybdate supported on alumina - is a typical hydrogenation catalyst with a very high hydrogenating activity. The reaction was studied at a pressure of 5.617 M Pa since thermodynamic considerations favour the reaction at high pressures. A bench-scale integral flow reactor, rather than a differential reactor, was used because of greater analytical accuracy.

CHAPTER 2

LITERATURE SURVEY

The hydrodenitrogenation (HDN) of pyridine is rapidly gaining importance from an industrial standpoint. As such, most of the literature available is rather recent. While many papers have been published on this subject, most researchers have studied the effect of promoters and modifiers on the conversion of pyridine to piperidine, often in a batch system. But, for a few investigations, the kinetics and mechanism of the reaction have been ignored.

Workers in the field generally agree that:

a) The hydrogenation of pyridine to piperidine is first order in pyridine, and

b) Serious deviation from first-order kinetics is observed in that the apparent first-order "rate constant" appears to be dependent on the initial pyridine content of the feed.

There is little agreement on the order in hydrogen and on the mechanism governing the conversion of piperidine to pentane and ammonia. Several mechanisms have been hypothesized ranging from very elementary[4] to rather complex ones[9].

The present survey deals mainly with the literature concerning the reaction kinetics and mechanism of the HDN of pyridine.

Cox[1] studied the destructive hydrogenation of pyridine over a catalyst containing 2.5% CoO and 14% MoO_3 supported on alumina. A first order in pyridine was observed wherein the reaction rate constant seemed to depend on the initial pyridine partial pressure.

Somers[2] found the rate to be first order in nitrogen content and first order in hydrogen partial pressure. The data was fitted with a Langmuir-Hinshelwood model which accounted for a decrease in the apparent first-order rate constant with increasing feed nitrogen content.

Rosenheimer and Kiovsky[3] found the denitrification of diesel fuel to be first order in nitrogen content and second order in hydrogen partial pressure.

McIlvried[4] studied the reaction over a presulfided catalyst containing 2.25% nickel, 1.25% cobalt, and 11% molybdenum. A fixed-bed flow reactor was employed. The feed (pyridine and piperidine) was dissolved in xylene. The catalyst was presulfided at 316°C and atmospheric pressure. The nitrogen-containing feed (nitrogen content varying from 100 ppm to 5115 ppm) was then passed over the catalyst at 316°C and pressures ranging from 5.27 M Pa to 11.54 M Pa. The apparent first-order rate constant for piperidine denitrification was reported to vary from 12.0 hr^{-1} to 1.0 hr^{-1} for feed nitrogen contents of 100 ppm and 4200 ppm respectively. Based on these observations, a rate expression for piperidine hydrogenation was developed:

$$r = k_n P_N P_H / (1+K_N P_N+K_A P_A)$$

where r is reaction rate,

k_n is piperidine denitrification rate constant,

P_N, P_H, P_A are partial pressures of pyridine, hydrogen and ammonia respectively,

K_N, K_A are adsorption coefficients of pyridine and ammonia respectively on hydrogen sites.

This rate expression assumes that the only substances adsorbed strongly

on the active sites are pyridine and ammonia. The constants were evaluated by integrating this equation and subjecting it to a least squares fit. A rate expression for pyridine hydrogenation was also developed. In order to allow for increased inhibition with conversion, it was assumed that one of the products, specifically ammonia, was more strongly adsorbed on the hydrogenation sites than the reactant but that they were equally strongly adsorbed on the denitrification sites.

It was concluded that the HDN of pyridine proceeds through three steps:

i) rapid hydrogenation of pyridine to piperidine;

ii) slow ring rupture to form n-pentylamine;

iii) rapid denitrification of n-pentylamine to give ammonia and pentane.

Extensive work has been carried out on HDN over MoO_3-Al_2O_3 and CoO-MoO_3-Al_2O_3[5-9]. Sonnemans, Goudriaan, and Mars[6] have reported that while the 4% CoO-12% MoO_3-Al_2O_3 catalyst had an activity and selectivity pattern similar to that of 22% MoO_3-Al_2O_3, the activity of the latter catalyst declined by about 25% after 50 hours while that of the cobalt-molybdate catalyst showed no decline.

Sonnemans et al[7] studied the hydrogenation of pyridine to piperidine over the above-mentioned catalysts in a high pressure flow system. With a hydrogen partial pressure of 6.0 M Pa, a first order in pyridine was observed. Changing the initial partial pressure of pyridine showed a deviation from first-order behaviour in that increased conversion of pyridine was observed at decreasing initial pyridine partial pressures. The first-order rate constant of the pyridine hydrogenation was found to be inversely proportional to the initial pyridine

partial pressure, an observation made by McIlvried[4] also. It was found that the order in hydrogen varied with temperature - from 1.0 at 250°C to 1.5 at temperatures greater than 300°C. They also used a rate expression assuming equally strong adsorption of pyridine and piperidine and a reaction rate constant depending on the initial pyridine partial pressure.

In another study, Sonnemans, Neyens and Mars[9] studied the conversion of piperidine. At temperatures below 325°C, selective conversion to N-n-pentylpiperidine and ammonia was observed. At higher temperatures, increasing amounts of pentane and ammonia with small amounts of pentylamine and pyridine were found. A very low order in piperidine was observed. Based on the large amount of pentylpiperidine formed, it was concluded that:

i) Piperidine is converted into ammonia, pentane, and pyridine and that pentylpiperidine is an intermediate in the formation of ammonia.

ii) Pentylpiperidine is converted into ammonia and pentane. Piperidine, pentylamine, and dipentylamine are intermediate products. A reaction mechanism was proposed and the rate constants were evaluated by computer simulation.

Satterfield et al[10,11] have studied the interaction between hydrodesulfurization (HDS) of thiophene and HDN of pyridine over commercial catalysts consisting of $CoMo/Al_2O_3$, $NiMo/Al_2O_3$, NiW/Al_2O_3, and $NiW/SiO_2-Al_2O_3$ at relatively lower pressures of 0.44 and 1.12 M Pa. It was observed that pyridine inhibited the HDS of thiophene. The sulfur compounds had a twofold effect on HDN. At low temperatures, they inhibited the rate of hydrogenation of pyridine while at higher temper-

atures, the hydrogen sulfide formed in the HDS reaction interacted with the catalyst to improve the catalytic activity. The inhibition of the HDS reaction was explained in terms of a two-site model. It was suggested that there are two types of active sites capable of catalyzing the HDS reaction:

Type I, which are very active and are responsible for the majority of HDS activity with pure thiophene feedstocks but are extremely sensitive to basic nitrogen compounds. In the presence of sufficient quantities of pyridine, these sites get completely blocked and are thus unavailable for HDS.

Type II, which have less HDS activity but are also less susceptible to poisoning, and therefore are responsible for the HDS activity after all Type I sites are blocked.

The twofold (temperature dependent) effect of sulfur compounds on HDN was not fully explained. It was suggested that below 325°C thiophene and the hydrogen sulfide formed during the course of the reaction compete for hydrogenation sites on the catalyst thereby slowing down the hydrogenation of pyridine. The increase in HDN activity at higher temperatures was attributed to several possible factors. Among them were the effect of the acidic nature of hydrogen sulfide on the catalyst surface thereby making it easier for the nitrogen compounds to be desorbed, possible stripping of the catalyst surface by hydrogen, causing a loss in the concentration of sulfur compounds on the surface.

Satterfield et al[12,13] have studied the thermodynamic equilibrium limitation on the formation of piperidine as an intermediate in the HDN of pyridine. A reversible reaction was assumed:

$$C_5H_5N + 3H_2 \rightleftharpoons C_5H_{11}N$$

It was found that in the presence of a large excess of hydrogen equilibrium towards piperidine became less favourable at higher temperatures and lower hydrogen pressures. At a total pressure of 1.12 M Pa, over $NiMo/Al_2O_3$ and $CoMo/Al_2O_3$ catalysts, it was observed that the equilibrium, which was far towards piperidine (≈100%) started moving towards pyridine in the vicinity of 300°C. Equilibrium data was also calculated from thermodynamic considerations. The calculated equilibrium supported the experimental values. The calculated equilibrium starts shifting towards pyridine at a temperature of about 250°C.

The calculated equilibrium at a hydrogen partial pressure of 10.0 M Pa also favours the formation of piperidine almost exclusively until about 360°C when it starts favouring pyridine. From this, Satterfield et al concluded that under certain conditions (low pressure and high temperature), the thermodynamic equilibrium between pyridine and piperidine could control the rate of HDN of pyridine.

Baltz[14] et al have studied the hydrogenation of pyridine to piperidine over $Co-Al_2O_3$ and $Co-Ni-Al_2O_3$ catalysts. At 150°C and pressures ranging from 15.0 to 22.0 M Pa, a product containing 99% piperidine, 0.6% pyridine and 0.4% byproducts was obtained.

Katzer et al[15] have studied the HDN and HDS of white oil. While studying the phenomena of catalyst poisoning, it was found that the poison largely responsible for the loss of catalyst activity was iron sulfide. Smaller amounts of Cu, Si, Al, Zn and Ti were also found to be present. It was also observed that deactivation occurred mainly at the front of the reactor where 50-70% of the catalyst surface was covered with a crust. A reduction in the poisoning of the catalyst was achieved by injecting the feed in the middle of the catalyst bed,

which was already at the reaction temperature.

Chegolya et al[16] studied the liquid phase hydrogenation of pyridine over ruthenium catalysts supported on alumina. A shaken, heated autoclave was used. The activation energy was reported to lie between 15 and 16 k cal/mole.

Dyukareva[17] studied the hydrogenation of pyridine over a nickel-aluminum alloy containing ruthenium in a batch system as well as a flow system. A catalyst life of 36 to 120 hours was reported, depending on the operating conditions.

Smeykal and Moll[18] studied the hydrogenation of pyridine containing 3-8% sulfur. Four catalysts containing combinations of nickel, tungsten, molybdenum and chromium supported on alumina were used. The presence of sulfur inhibited the conversion of pyridine. If the pyridine was desulfurized, a larger conversion was obtained at relatively milder operating conditions.

Several investigators have studied the hydrogenation of pyridine over Raney nickel using different promotors and modifiers[19-24]. An increase in catalytic activity was reported in all cases.

Madkour et al[25] reported an increase in the activity of cobalt-molybdenum catalyst supported on alumina upon modification with hydrogen chloride while investigating the hydrogenation of quinoline.

Beugeling et al[26] developed a stationary phase for the separation of the products of pyridine hydrogenolysis. Column packings made of chromosorb W, acid washed, 60-80 mesh, coated with 1% (W/W) NaOH in a methanolic solution and 10% (W/W) carbowax 1000 or OV-17 were found to be especially suitable. All the products of the HDN reaction could be separated and there was no significant tailing of the peaks. The NaOH

was said to have eliminated the problem of tailing because of its strong basicity.

The identified products included ammonia, n-pentane, n-pentane-1, n-decane, N-methylpiperidine, n-pentylamine, piperidine, n-butanecarbonitrile, N-n-pentylpiperidine, di-n-pentylamine and tri-n-pentylamine. It was also observed that using p-xylene as a solvent, products such as toluene and trans 1,4-dimethylcyclohexane were also formed. The retention times on different columns were determined.

A quantitative analysis was also conducted to obtain relative weight factors for some of the more important products. The values of the weight factors obtained in this study agreed very closely with those obtained by Dietz[27] except in the case of pentylamine. This was explained by possible decomposition of the pentylamine in the injector or the column.

CHAPTER 3

EXPERIMENTAL

A. Experimental Setup

A flow system, incorporating an integral flow reactor, was designed and set up for investigating the hydrodenitrogenation (HDN) of pyridine. Figure 1 is a schematic diagram of the apparatus. The apparatus may be considered to consist of three sections or zones:

1) feed zone
2) reaction zone
3) product analysis zone.

Since a gas (hydrogen) and a liquid (pyridine, n.b.p. 115°C) had to be mixed, the liquid had to be vaporized. The gas, therefore, had to be preheated prior to coming in contact with the liquid, to prevent condensation of the liquid in the tubes, all the tubing downstream of the mixing point was maintained at an elevated temperature by wrapping the lines with electrical heating tape (Electrothermal Engineering Limited). In order to reduce the heat losses to the atmosphere, the heated lines were insulated with 1/8 inch thick asbestos tape. The material of construction of the apparatus is type 316 stainless steel throughout, unless otherwise specified.

1. Feed Section

Hydrogen gas was obtained from a high pressure cylinder through a high pressure, spring-loaded regulator (Matheson, model 3, delivery pressure range 689 k Pa - 10.34 M Pa, brass body, stainless steel diaphragm, nylon seat). The gas, drawn from the regulator at 5.617 M Pa, was passed through a drying tube packed with anhydrous calcium sulfate.

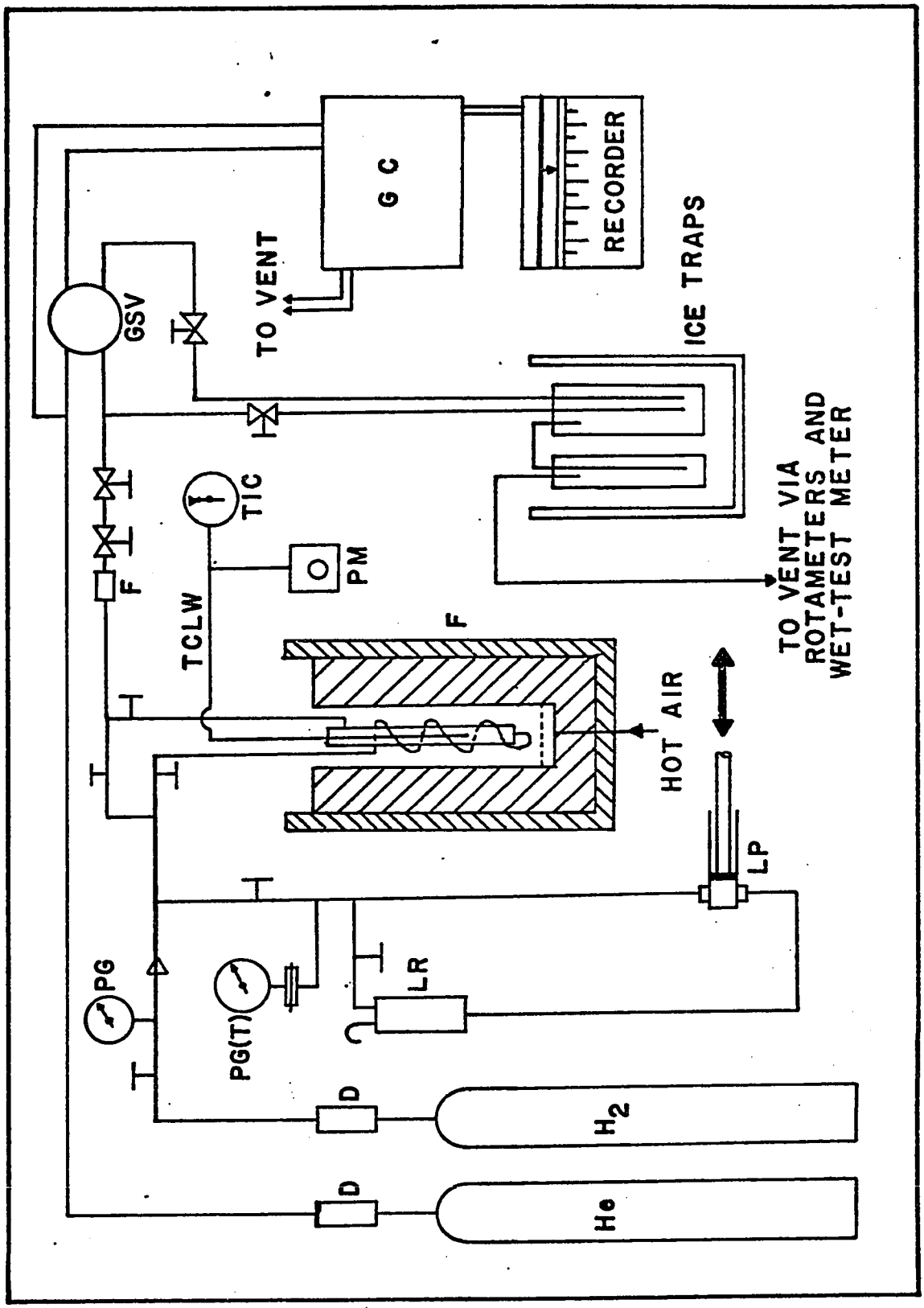

FIG·1: EXPERIMENTAL SETUP

LEGEND FOR FIGURE 1

D:	drier tube
F:	filter
GC:	gas chromatograph
GSV:	gas sampling valve
LP:	liquid pump
LR:	liquid reservoir
PG:	pressure gauge
PG(T):	pressure gauge (test)
PM:	potentiometer
TCLW:	thermocouple lead wires
TIC:	temperature indicator-controller

The gas feed line was constructed from 6.35 mm O.D. (3.9 mm I.D.) tube. The dried gas passed through a shut-off valve (Whitey Co., Oakland, Cal., union bonnet), past a pressure gauge (Matheson, 0-6.89 M Pa), and through a check valve (Matheson). The gas next passed through a preheating zone prior to coming in contact with the liquid. The preheating zone comprised 1 m. of the tube carrying the gas wrapped in heating tape. The gas then entered one branch of a union tee (Swagelok Company, Cleveland, Ohio).

The liquid was fed using a reciprocating, positive-displacement minipump (Milton Roy Company, Riviera Beach, Florida). The pump consisted of three major parts: a drive unit, plunger, and liquid end. The drive unit consisted of an electrical motor and a reduction gear assembly to give 31 plunger strokes per minute. The plunger was made of sapphire and was 3.175 mm diameter. The maximum stroke of the plunger was 12.7 mm. The discharge rate could be varied by adjusting the plunger stroke with the help of a micrometer. The liquid end consisted of dual ball check valves in series on the suction and discharge sides. The ball checks and ball seats were made of sapphire, the ball guides of Kel-F, the ball stops of ceramic and the plunger seal and plunger back-up ring were made of carbon filled Teflon and Hastelloy C. The liquid end was housed in a Carpenter 20 stainless steel casing.

The minipump was rated to 6.90 M Pa and the discharge could be varied from 16 to 160 cu.cm./hr. with a repetitive accuracy of ±0.3% at pressures above 690 k Pa. Lower discharge rates could be obtained with a negligible loss of accuracy.

The intake to the pump was from a liquid reservoir vented to the atmosphere. The reservoir was filled with pyridine, as required. On the high pressure end of the pump, an oil-filled, diaphragm type test gauge

(0-10.3 M Pa, 34.5 k Pa subdivisions) was attached. The liquid passed through a shut-off valve (Autoclave Engineering Inc., Eric, Pa.) and a bypass valve, and entered the second branch of the union tee. Pyridine vaporized upon contact with the hot gas and the hot walls of the fitting. Downstream of this point, all the lines were heated and insulated.

The reactant mixture next went to a three-way valve (Autoclave) which was used to either direct the reactants to the reactor or to bypass the reactor.

2. Reactor Zone

The reactor consisted of a 20.5 cm. long stainless steel tube, 12.5 mm O.D.,1.1mm wall thickness, filled with catalyst particles (-20, +40 mesh size). The catalyst bed was supported on a porous stainless steel plate (grade D plate with a mean pore size of 65 microns, a normal thickness of 1/16 in., and which produced a pressure drop of 689 Pa at 5.5 ℓ/cm^2-min. of air, supplied by Pall Trinity Micro Corporation, Cortland, New York). A thermocouple (type J, sheathed in a 3.175 mm O.D. stainless steel casing, sealed) was inserted in the catalyst bed, the tip of the thermocouple being 6 cm. above the porous plate supporting the catalyst bed. As the quantity of the catalyst used was constant throughout the experiments, the height of the catalyst bed was always constant at about 15 cm. Thus, the distance of the tip of the thermocouple from the bottom of the catalyst bed was about 40% of the height of the catalyst bed. The empty space above the catalyst bed was packed with glass wool to prevent the catalyst particles from being carried away by the gas stream.

The reactants, from the three-way valve, entered a preheating zone (see Figure 2) comprising a 3.175 mm O.D. (1.4 mm I.D.)

tube wound loosely around the reactor. The purpose of the preheater was to bring the reactants to the same temperature as the catalyst bed, thereby reducing thermal gradients in the reactor. The reactants entered the reactor from the bottom, passed through the catalyst bed and the products were drawn from the top of the reactor. The product stream passed through a stainless steel filter (Nupro Company, Cleveland, Ohio with stainless steel element, 15 microns) used to protect the downstream equipment from contamination, dirt, and strands of fiberglass that could possibly disengage in the reactor and get carried away by the product stream.

The reactor was placed in a furnace comprising an aluminum cylinder, 10 cm. O.D. x 4 mm. thickness x 40 cm. long, filled with sand. The sand rested on a porous stainless steel plate which also served as a distributor for the hot air used to fluidize the bed. The air was heated by wrapping the air-carrying copper tube with electrical heating tape. The air flow rate could be adjusted.

There were five strip heaters attached to the outside of the aluminum cylinders. Three of these heaters were in parallel and were kept in an 'ON' position at all times. The other two heaters were powered by a temperature controller (Honeywell, model 7350, type J, 0-650°C). The power input into the two banks of heaters was varied depending on the required reactor temperature. The feedback into the controller was from the thermocouple inserted in the catalyst bed. The controller was a cyclic on-off type, thereby performing as a proportional controller. As such, the controller worked with an 'offset' but did not cause the temperature to 'hunt' around the set point, a phenomena generally encountered while using simple on-off mode of control.

The heater assembly was placed in a larger aluminum cylinder and the annular space was filled with insulating materials. The furnace was further insulated on the outside by asbestos.

The thermocouple immersed in the catalyst bed was also used for measuring the temperature using a potentiometer.

Next, the pressure of the product stream was reduced to 142.7 k Pa by means of two needle valves in series (Whitey, union bonnet regulating, maximum coefficient of discharge, C_V = 0.37, and Nupro, fine metering, maximum C_V = 0.0040).

The product stream was next split into two fractions, A and B. Stream A went directly to two ice-traps (in series) while stream B passed through a gas sampling valve and then met stream A in the ice-traps. Metering valves (Autoclave) were installed so as to vary the relative flow rates of streams A and B, and to regulate the pressure in the sample loops as required.

After trapping the condensables in the ice-traps, the gas stream passed through three rotameters (Matheson 601, maximum hydrogen flow: 550 std.cu.cm./min.; Matheson 602, maximum hydrogen flow: 2300 std.cu.cm./min.; and Matheson 73, maximum hydrogen flow rate: 5800 std.cu.cm./min. with glass float and about 15000 std.cu.cm./min. with steel float) in parallel. The gas stream could be diverted to any of the flow meters by means of shut-off valves on the inlet side of each rotameter. Depending upon the hydrogen flow rate needed, an appropriate rotameter was used.

To guard against erroneous rotameter readings because of fouling of the tubes or the floats, the gas stream was then led to a wet-test meter. The instantaneous flow rate shown by the rotameter was checked periodically with the cumulative flow rate shown by the wet-test meter,

and very close agreement between the two was observed.

3. Analysis Section

In this section, a sample was drawn from the product stream by means of a gas sampling valve (Hewlett Packard, model 19021A) and analyzed on a gas chromatograph (Hewlett Packard, model 5750 Research Gas Chromatograph). The products were identified using a thermal-conductivity detector and the results were recorded on a strip chart recorder (Hewlett Packard, model 7127A).

The product stream entered and left the sampling valve continuously through heated lines. The sampling valve was thermostated at 170°C and was enclosed in an insulated chamber and mounted on the chromatograph. The sampling valve assembly was of the rotary shear-force type and employed a filled Teflon rotor against a polished stainless steel seat. The seat had eight ports which provided for dual sampling loops. The dual loop configuration had the advantage of allowing one loop to be purged and filled while the second loop was being used. Each of the matched loops had a volume of 0.5 cu.cm. including the internal volume of the valve. The valve could be thermostated to 200°C and was rated to have no leakage across ports at pressures ranging from 1 mm Hg to 1.38 M Pa.

The chromatograph comprised an oven for the columns, a detector cell, a power supply unit for the detectors, a recorder for recording the output from the detectors and associated plumbing and electronics.

The oven contained two identical columns (copper, 4 mm I.D. x 6 m. long, packed with Chromosorb W coated with 1% NaOH and 10% Carbowax). While one of these served as an analytical column, the other one was the

reference column. The carrier gas, helium, was drawn from a high pressure cylinder at 552 k Pa by means of a regulator (Matheson, two-stage) and passed through a drying tube packed with anhydrous calcium sulfate. In the oven module, it was split into two streams - the reference stream and the analytical stream - and passed through two matched rotameters with fine metering valves. The reference stream went directly to the reference column while the analytical stream entered the sampling valve and then went to the analytical column. The column oven temperature could be programmed at a linear rate varying between 1°C/min. and 60°C/min..

The two streams next went to a thermal conductivity detector assembly where they were compared. The output from the detectors was recorded on a single channel, high resolution recorder, with a full scale range of 1 mV.

B. Catalyst, Chemicals and Reactants

Specifications of chemicals used are as follows:

1. Catalyst

The catalyst was 3% CoO-15% MoO_3-Al_2O_3 (Harshaw Chemical Company). It was supplied kindly by the Department of Energy, Mines, and Resources, Ottawa, Ontario. The catalyst was obtained in the form of 1/8 in. diameter extrudate. It was crushed and sieved, and the -20, +40 mesh size fraction (average particle diameter 0.63 mm) was used. Surface area measurements were made at the Energy Research Laboratories of the Department of Energy, Mines and Resources by means of nitrogen adsorption and the following results were obtained.

On "as received" basis, the surface area was found to be 203

sq.m./gm.

On degassed (moisture-free) basis, the surface area was found to be 214 sq.m./gm. The bulk density of the 1/8 in. extrudate was 0.60 gm/mℓ and that of the -20,+40 mesh size employed in this study was 0.792 gm/mℓ.

A sample of a similar catalyst (4% CoO-12% MoO_3-Al_2O_3, Ketjen, Amsterdam; supplied by the Department of Energy, Mines and Resources, Ottawa, Ontario) was obtained. Both samples were submitted to the Analytical Section, Division of Chemistry, National Research Council of Canada, Ottawa, Ontario) for spectrographic analysis. The analysis was carried out by Mr. P. Tymchuk. The results of the analysis are as follows:

Results of spectrographic analysis

a) Values accurate to ±20%

ELEMENTS	HARSHAW CATALYST	KETJEN CATALYST
Co as Co_3O_4	2.5%	2.5%
Mo as MoO_3	14.5%	12.0%
Si as SiO_2	approx. 0.01%	2.0%
Na as Na_2CO_3	none visible: <0.2%	0.3 to 1%
Fe as Fe_2O_3	none visible	approx. 0.015%

Semi-quantitative values - within a factor of 3.

Ni	0.15%	0.05%
Cu	0.01%	0.001%
Ti	0.1%	0.02%
Mg	0.005%	0.01%
Mn	0.01%	0.02%

2. Chemicals and reactants

Pyridine: C_5H_5N, Fisher Scientific Company, "Certified Grade", Lot No. 763891. Lot analysis:

Water: 0.05%

Chloride: 0.0003%

Sulfate: 0.0003%

Ammonia: 0.001%

Boiling Point: 115.3°C ± 0.1°C

Hydrogen: H_2, Liquid Carbonic Canada Ltd., 99.95% minimum purity.

Helium: He, Liquid Carbonic Canada Ltd., 99.95% minimum purity.

Piperidine: $C_5H_{11}N$, Fisher Scientific Company, "Certified Grade", Lot 751792, 0.1% water.

Pentylamine: $C_5H_{13}N$, Eastman Kodak Company, Rochester, New York, Lot D6A.

Dipentylamine: $C_{10}H_{23}N$, Eastman Kodak Company, Rochester, New York, Lot 692-1B.

Pentane: C_5H_{12}, Fisher Scientific Company, "Certified, Infra Red Spectranalyzed".

Ammonia: NH_3, Matheson of Canada, 99.99% minimum purity.

3. Column Packing

Stationary Phase: Chromosorb W, Chromatographic Specialties Limited, acid-washed, -60,+80 mesh size, Lot 484.

Liquid Phase: Carbowax 1000, Chromatographic Specialties Limited, NaOH; chemically pure.

Solvents: Methanol, CH_3OH, and methylene chloride, CH_2Cl_2, Fisher Scientific Company, "Certified" grade.

C. Experimental Procedure

For the sake of clarity, the experimental procedure may be said to comprise of four phases.

1. Installation and pressure test

Upon initial installation, the apparatus was tested for leakage at the operating pressure. The setup was initially pressurized with helium at 1.48 M Pa. All the fittings were tested with a liquid leak detector until the system could sustain pressure when isolated. The pressure was then raised to 7.0 M Pa and checked for leakages until there was no pressure drop on isolation for about 4 hours. The apparatus was then vented and filled with hydrogen to 5.617 M Pa. Having observed no evidence of leakage, the lines werewrapped in heating tape and insulated with asbestos.

During the course of the experiments, periodic checks for leakage were made. If leakage was observed, it was located and the cause of the leakage was removed (generally worn out sleeves, fittings, glands, etc.).

2. Column preparation and conditioning

The columns were packed with Chromosorb W (acid-washed, -60,+80 mesh size) coated with 1% (W/W) NaOH and 10% (W/W) Carbowax 1000. Required amounts of the liquid phase, NaOH, and the stationary phase were weighed. NaOH was dissolved in methanol and the solution poured onto the Chromosorb in a shallow porcelain dish. It was dried at room temperature with frequent stirring until the material regained its powdery form. A solution of the Carbowax in methylene chloride was then poured on the Chromosorb and the resulting slurry dried as before.

Two 6 m. lengths of copper tubing (6.35 mm O.D.) were then packed with this material using a vibrator. The ends were stuffed with glass-wool and the columns were bent into coils of convenient size and shape so that they would fit in the oven. Helium flow through the columns was started (with the detector disconnected) and the oven temperature raised to 145°C for conditioning. After 48 hours, the oven was cooled down and the columns were connected to the detectors.

3. Calibration

The flowmeters and the liquid pump were calibrated next. The rotameters were calibrated by passing hydrogen gas through them at 20°C and atmospheric pressure (±10 mm water). The rotameter reading was noted and the flow was measured using a soap-bubble meter or a wet-test meter, the latter for higher flow rates.

The liquid pump was calibrated by installing a graduated pipet on the suction side of the pump and measuring the discharge rate at an upstream pressure of 5.62 M Pa.

The chromatograph was calibrated in two stages - qualitatively and quantitatively. The first step comprised of injection of pure compounds and noting the time of elution of different compounds. These times were matched with the elution times of the products formed by reaction and the products formed were identified.

Mixtures of known composition containing the identified reaction products were prepared and injected on the chromatograph. The area under the peaks (one for each compound) was computed by measuring the base and height of each peak and corrected for sensitivity and chart speed. By repeating these runs over a wide range of compositions, relative weight

factors were calculated for each compound (relative to piperidine). These were found to be constant for each compound and showed good agreement with relative weight factors calculated from the work of Beugeling et al[26] and Dietz[27].

4. Startup and operation

A weighed quantity of crushed and sieved catalyst (constant throughout this investigation at 10.365 gms, -20,+40 mesh size) was loaded into the reactor. The reactor was fitted in place and pressure tested. The apparatus was pressurized with hydrogen and a low flow rate (about 300 std.c.c./min) established. Heaters for the furnace were switched to the 'ON' position and the electrical heating tape was also energized. The reactor temperature controller was set at 440°C and the reactor maintained at that temperature for 48 hours for reducing the catalyst. It was then cooled to about 150°C. Hydrogen and pyridine flow rates were then established and maintained continuously and a sample of the product stream analyzed every 8-10 hours until a constant product distribution was obtained indicating that the catalyst had been conditioned and its activity had stabilized. The system was now ready for an experimental run.

A residence time and a reactant ratio were chosen and the hydrogen and pyridine flow rates calculated. The reactor was brought to the desired temperature and the reactant flow rates adjusted to the calculated values. The temperature of the catalyst bed was monitored via the potentiometer and was maintained constant. Samples of the product stream were analyzed every 45 minutes until at least three successive analyses were identical, indicating thereby that steady state had been attained.

The reaction conditions were then changed to the ones required for the next reading.

The reservoir at the suction side of the pump was filled and the ice-traps drained as required. During the course of the actual experimental work, no daily overnight shut-off procedure was observed, i.e. the equipment was run continuously. However, for extended shut-offs, the pyridine flow was stopped and the hydrogen flow was reduced but the pressure over the catalyst was maintained at 5.617 M Pa.

The activity of the catalyst was checked once a week by operating at conditions for which the conversion was known. Whenever a change in the catalyst activity was observed, the catalyst charge was replaced with a fresh load and the readings taken since the last satisfactory catalyst activity test were repeated.

Fouling of the rotameters was indicated by a discrepancy in the flow rate indicated by the rotameters and the rate calculated from the cumulative flow measured by the wet-test meter. In such an event, opening and cleaning of the rotameter tube and float with acetone was very helpful.

CHAPTER 4

THEORY

Modern theories of heterogeneous catalysis postulate that the catalyst must play some role in the intermediate steps during the course of a reaction, even though it does not appear to be an initial reactant or a final product of the reaction. During these intermediate steps, the catalyst somehow changes, energizes, or otherwise affects the reactants to form intermediates. One theory views the intermediate to be an association of a reactant molecule with a region of the catalyst surface while another theory assumes the reactant molecules move down into the atmosphere close to the catalyst surface where the molecules are still mobile but are affected by surface forces. Yet another theory postulates the formation of an activated complex or a free radical at the catalyst surface. The free radical then moves back into the bulk gas stream, triggering a chain of reactions with fresh molecules before being finally destroyed. In contrast with the first two theories which consider the reaction to occur in the vicinity of the catalyst surface, the third theory views the catalyst surface simply as a source of free radicals, with the reaction taking place in the bulk phase.

In terms of the transition state theory, the catalyst may be said to substitute a sequence of steps, each having a lower activation energy, for the high-activation energy single step uncatalyzed reaction. This is generally brought about by the formation of an activated complex.

An important feature of catalyzed reactions is that a catalyst which accelerates the forward reaction in an equilibrium system is a catalyst

for the reverse reaction too. Thus, the catalyst has no effect on the equilibrium conversion, which is governed by thermodynamics alone. Rather, the catalyst would generally affect the rate of attainment of equilibrium.

A. Rate Steps in Heterogeneous Catalysis

A catalytic reaction occurs in several steps, each offering a certain resistance to the overall reaction. The sequence of steps is as follows[28]:

1. Transport of the reactants from the bulk phase to the catalyst surface.
2. Diffusion of reactants into the pores of the catalyst (for porous catalysts).
3. Adsorption of reactants on the interior sites of the catalyst particle.
4. Chemical reaction of adsorbed reactants to adsorbed products.
5. Desorption of the adsorbed products.
6. Diffusion of products from the pores of the catalyst to the catalyst surface (for porous catalysts).
7. Transport of products from the catalyst surface to the bulk phase.

Since these steps occur in series, the rate of each of these steps is equal to the overall rate at steady state. This equality is the basis for the development of the concept of global reaction rates in terms of the bulk phase concentration and temperature. This concept assumes great significance because it is impossible to measure the temperaturesand pressures on the catalyst surface and in the interior of

the catalyst pore with any degree of accuracy.

Steps 1, 2, 6 and 7 are physical steps. They can be controlled at will and accounted for independently. Steps 3, 4 and 5 are chemical steps and hence are of more significance. Generally, the resistance offered by one or two of these steps is much greater than that offered by the third one, and as such, the step that offers the largest resistance can be said to be rate-controlling.

B. External Mass and Heat Transfer

While correlating experimental data to theoretical rate equations, the temperature and partial pressure terms employed should, strictly speaking, be measured at the catalyst surface. The degree of error involved in using the bulk phase properties are minimal in fluidized bed reactors. In fixed bed reactors, however, large temperature and pressure gradients can exist between the bulk phase and the solid-fluid interface. As such, it is highly desirable, in a fixed bed experimental study, to operate at conditions that give rise to high heat and mass transfer coefficients. It can then be assumed that the bulk phase properties bear a very high degree of proximity to the properties at the interfaces.

Partial pressure and temperature gradients have been calculated by the method of Yoshida et al[29] and the results are given in Appendix D.

C. Internal Mass and Heat Transfer

Two kinds of diffusion take place inside the pore, depending on whether the diffusing molecule is likely to encounter another molecule or the pore wall. It follows, then, that the nature of diffusion inside

the pores depends on the relative magnitude of the mean free-path of the reactant and the pore size.

i) Molecular diffusion

Molecular, or bulk, diffusion is likely to predominate if the mean pore size is very large as compared to the mean free path of the diffusing molecules. This can be avoided by working in a region of high superficial velocity. If molecular diffusion is significant, an increased flow rate (at constant space-velocity) results in increased conversion. The effect of bulk diffusion was estimated by measuring the conversion at different flow rates (all other parameters being constant) and the results are given in Appendix E.

ii) Pore diffusion

Pore, or Knudson, diffusion is encountered if the mean pore size is small compared to the mean free path of the diffusing substance. If pore diffusion is significant, a reduction in the catalyst particle size results in increased conversion. This can be avoided by using a small catalyst particle size. The extent of pore diffusion can be estimated by measuring the conversion using catalyst particles of different sizes. The results are given in Appendix E.

D. Determination of Rate-Controlling Step

Having minimized the effect of steps 1, 2, 6 and 7, we are now left with the three chemical steps viz. adsorption of the reactants onto the catalyst, surface reaction, and desorption of the products from the catalyst pores. Out of these three steps, the rate controlling step is to be determined. This is done by varying the partial pressure of one of the reactants (by varying the total pressure and/or by changing the

feed composition) and correlating the initial rate data as described by Yang and Hougen[30]. They envisage the reaction rate to comprise of three terms viz. a kinetic term, a driving potential term, and an adsorption term. Thus,

$$\text{rate} = \frac{(\text{kinetic term}) \times (\text{driving potential term})}{(\text{adsorption term})^{m}}$$

Expressions for the three terms as well as values of m have been tabulated for different steps that could be encountered in four different types of reactions. A visual comparison of Figure 2 (initial rate vs initial pyridine partial pressure) with the six possible curves published by Yang et al[30] shows that adsorption of pyridine, with or without dissociation, is controlling. If pyridine is not dissociated, m, the exponent of the adsorption term has a value of 1 while if pyridine is dissociated, m assumes a value of 2, leading to a more complicated rate expression. As such, dissociation of pyridine is assumed in the development of the rate expression.

E. Development of the Rate Equation

For a reaction of the form

$$\underset{(Pyr)}{\text{Pyridine}} + \underset{(H)}{\text{Hydrogen}} \rightleftharpoons \underset{(Pip)}{\text{Piperidine}}$$

the three terms comprising the rate expression can be written as follows:

Driving potential term: $\left(a_{pyr} - \frac{a_{pip}}{K_e\, a_H}\right)$

Kinetic term: $(EL\, K_{pyr})$

Adsorption term: $\left(1 + \frac{K_{pyr}\, a_{pip}}{K_e\, a_H}\right)$

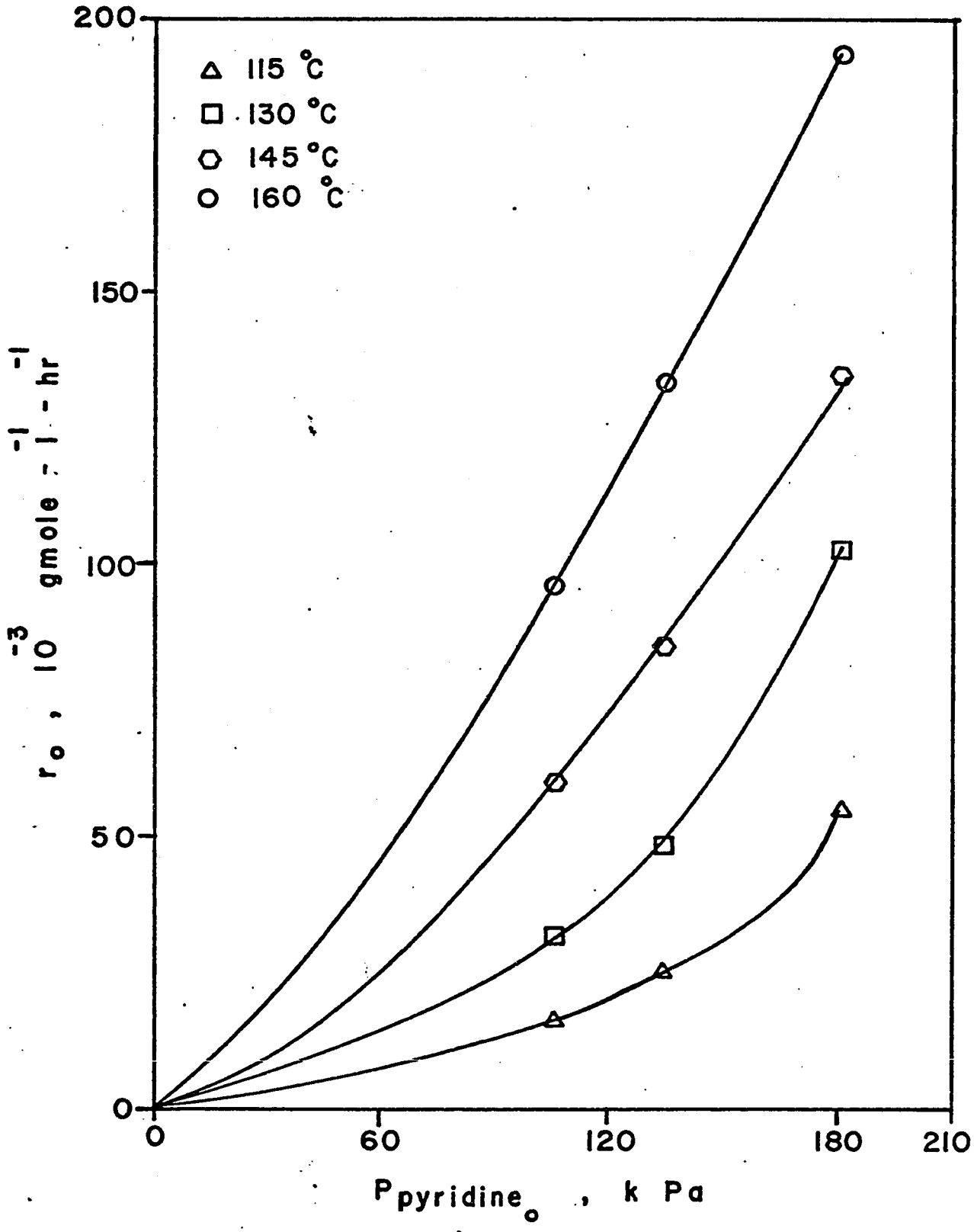

Fig. 2. Initial rate versus initial concentration.

m, exponent for adsorption term = 2

and the rate expression becomes

$$\text{rate} = \frac{\left(a_{pyr} - \frac{a_{pip}}{K_e a_H}\right) \times (EL\, k_{pyr})}{\left(1 + \frac{K_{pyr}\, a_{pip}}{K_e a_H}\right)^2} \qquad (5.1)$$

where a_{pyr}, a_H, a_{pip} are activities of pyridine, hydrogen, and piperidine respectively,

K_{pyr} is adsorption equilibrium constant for pyridine,

K_e is overall equilibrium constant,

k_{pyr} is reaction velocity constant for pyridine,

L is total number of active sites,

and E is the effectiveness factor.

Figure 3 (thermodynamic equilibrium between pyridine and piperidine in the presence of hydrogen, calculated by Satterfield et al[13]), shows that the equilibrium is far to the right. This means that K_e, the overall equilibrium constant, will have a very large magnitude. Furthermore, with a vast excess of hydrogen, a_H is also very large. Then, equation (5.1) simplifies to the form:

$$\text{rate} = EL\, k_{pyr}\, a_{pyr} \qquad (5.2)$$

since all the terms containing K_e in the denominator can be approximated as zero. In other words, the reaction which is theoretically reversible can be treated as irreversible.

The E, L and k_{pyr} are lumped together into a reaction rate constant K:

$$\text{rate} = K\, a_{pyr} \qquad (5.3)$$

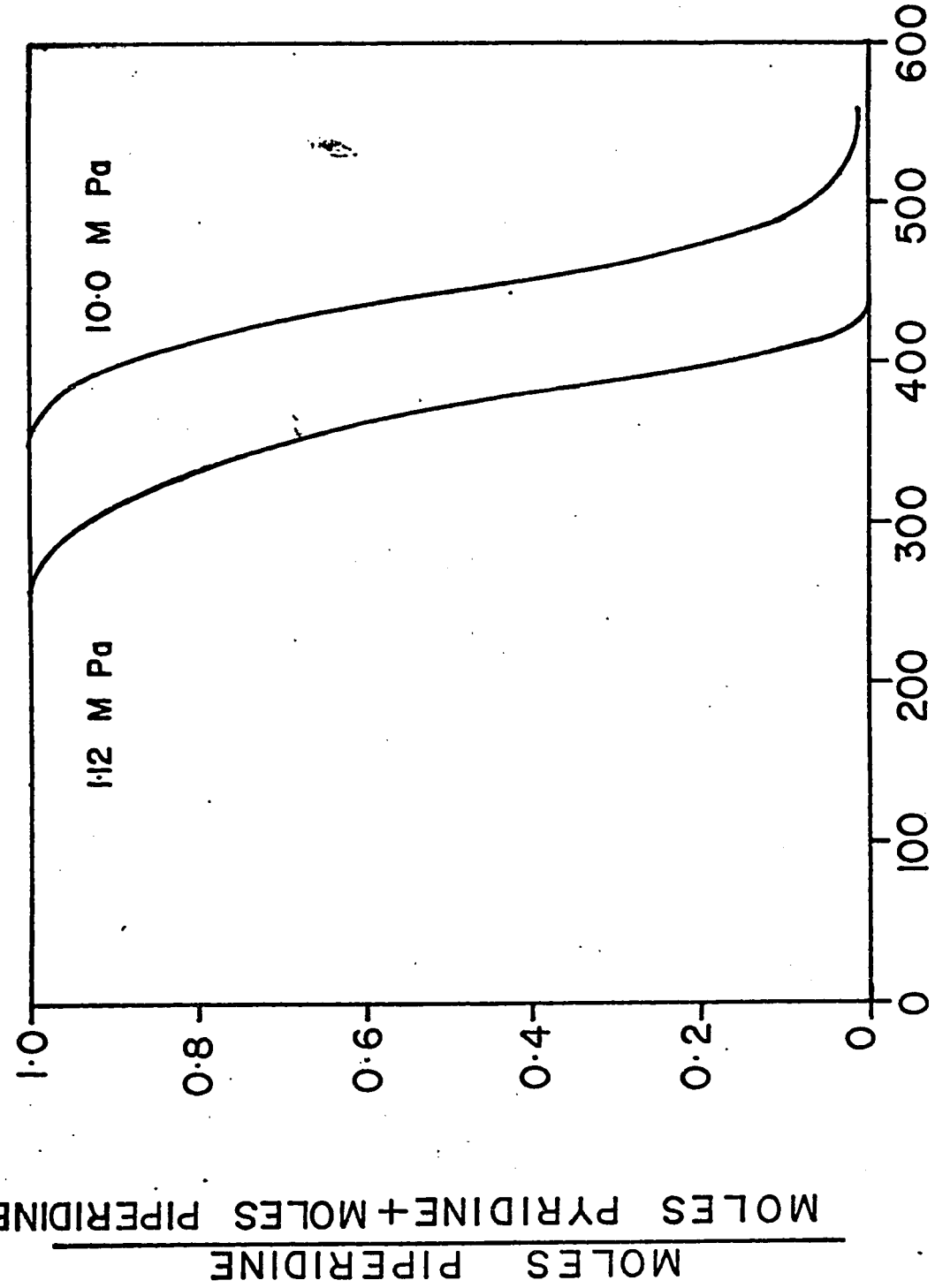

Fig. 3. Thermodynamic equilibrium of pyridine-hydrogen-piperidine[13].

The activity of pyridine, a_{pyr}, will be some function of the form:

$$a_{pyr} = (C_{pyr})^n \tag{5.4}$$

or, substituting into (5.3), we get

$$\text{rate} = K(C_{pyr})^n \tag{5.5}$$

where C_{pyr} is the concentration of pyridine

and n is the order of the reaction in pyridine.

F. Integration of the Rate Expression

The rate expression developed above can be applied to an elemental section of the reactor and integrated over the entire reactor volume. The following assumptions are made:

i) The velocity profile in the reactor is flat, i.e. plug flow exists. This can be justified by the presence of the fine (15 microns pore size) plate at the inlet to the reactor and by the fine particle size.

ii) The reactor operates isothermally, i.e. there are no thermal gradients in the reactor, either radial or axial. Theoretically, this assumption can never be valid if heat effects accompany the reaction since a finite thermal gradient is essential for removal or addition of heat. However, this ideal state is approximated by placing the reactor in a fluidized bed.

iii) There is no radial or axial dispersion in the reactor.

iv) The number of moles does not change during the course of the reaction. With a vast excess of hydrogen, this assumption is valid.

v) There is no pressure-drop across the length of the reactor.

For the sake of simplicity, rate of reaction, r, flow rate, F, and concentration C, all refer to pyridine. Subscripts o and f indicate initial and final conditions respectively.

Consider an element of the catalyst bed as shown.

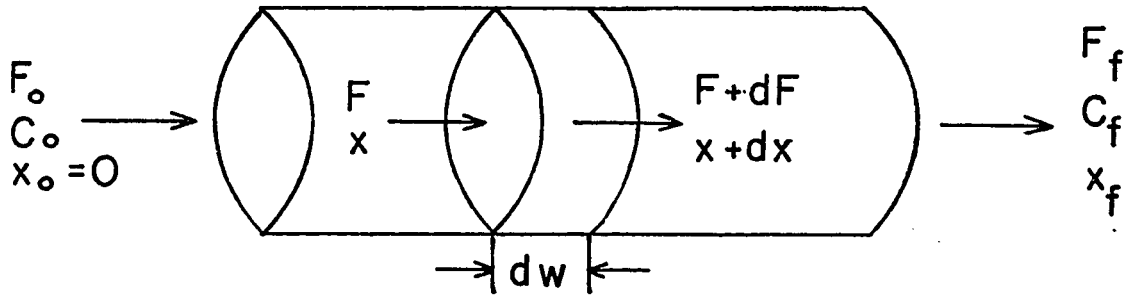

For an element of volume dW,

$$\text{Input} = F \tag{5.6}$$

$$\text{Output} = F + dF \tag{5.7}$$

$$\text{Disappearance by reaction} = -(r)dW \tag{5.8}$$

where the rate is defined as the number of moles reacting per unit time per unit catalyst volume.

$$\text{But, input} = \text{output} + \text{disappearance by reaction.} \tag{5.9}$$

Substituting (5.6), (5.7) and (5.8) in equation (5.9), we get

$$F = F + dF - r\,d\,W$$

or

$$dF = r\,d\,W \tag{5.10}$$

Defining fractional conversion x as

$$x \equiv \frac{F_o - F}{F_o} = \frac{C_o - C}{C_o}$$

we have

$$dF = - F_o \, dx \tag{5.11}$$

Substituting into (5.10), we have

$$- F_o \, dx = r \, d \, W \tag{5.12}$$

Separating the variables and integrating, we get

$$\int_o^W \frac{dW}{F_o} = - \int_o^x \frac{dx}{r}$$

or

$$\frac{W}{F_o} = - \int_o^x \frac{dx}{r}$$

$$= - \int_o^x \frac{dx}{K \, C^n} \tag{5.13}$$

Utilizing the definition of x, equation (5.13) can be integrated for different values of n to give:

$$n = 0: \quad C = C_o - K \frac{W}{F_o} \tag{5.14}$$

$$n = 1: \quad \ell n \left(\frac{C}{C_o}\right) = -K \frac{W}{F_o} \tag{5.15}$$

$$n = 2: \quad \frac{1}{C} - \frac{1}{C_o} = K \frac{W}{F_o} \tag{5.16}$$

Defining F in volume per unit time reduces $\frac{W}{F_o}$ to the units of time. This is the concept of residence time, t, based on the limiting reactant, pyridine in this case.

The instantaneous concentration C in equations (5.14) to (5.16) can be replaced by x to give:

$$\text{Zero order:} \qquad x = \frac{K\,t}{C_o} \tag{5.17}$$

$$\text{First order:} \qquad \ell n(1-x) = K\,t \tag{5.18}$$

$$\text{Second order:} \qquad \frac{x}{(1-x)} = K\,t \tag{5.19}$$

Experimentally obtained data of conversion vs residence time (Figures 11, 12 and 13) are now tested to determine which of the rate expressions fits the data. Equation (5.17) fits the data best and, as such, it was concluded that the reaction has an order of zero with respect to pyridine.

The equilibrium rate constant, K, is theoretically supposed to be a function of temperature only. However, it was found that the value of K changed with the initial starting partial pressure of pyridine. The dependence of K on C_o and T was delineated assuming the following relation:

$$K = K_p\,(C_o)^n \tag{5.20}$$

where K_p is a pseudo rate constant dependent only on temperature. Taking logarithms of equation (5.20), we get

$$\ell n\ K = \ell n\ K_p + n\ \ell n\ C_o \tag{5.21}$$

The value of n was found by means of a least-squares fitting program on an IBM 360 computer (see Appendix F).

Pseudo rate constants were now calculated and the activation energy found from Arrhenius' law:

$$K_p = k_o e^{-E_o/RT}$$

where k_o is the frequency factor or the pre-exponential factor,

e is base to natural logarithms,

E_o is the energy of activation, k calories

R is the universal gas constant,

$1.987 \text{ cal-gmole}^{-1}\text{-}^{\circ}\text{K}^{-1}$

T is the temperature, °K.

CHAPTER 5

RESULTS

The experimental work was carried out in a high-pressure isothermal, fixed-bed, integral reactor at 5.62 M Pa. All the measurements were made under steady state conditions. No attempts were made to study the dynamics of the reactor. In order to simplify the treatment, ideal conditions were approximated. Suitable assumptions were made, where applicable.

Conversion has been defined as the number of moles of pyridine reacted per mole of pyridine fed into the reactor.

The residence time, W/F, or t, has been calculated on the basis of the feed rate of the limiting reactant, pyridine in this case, and considering it to be completely vaporized. The pyridine liquid flow rate was converted to a volumetric vapour flow rate (using ideal gas law) and corrected for the pressure prevailing in the reactor. No correction was made for the temperature. To obtain more relevant units of the residence time, the catalyst quantity was taken in cu.cm. (mass of the catalyst divided by its bulk density) as opposed to the conventional method of taking the catalyst quantity in terms of its mass. The units of residence time then turn out to be $[T]$. The catalyst quantity was maintained at 10.365 gms. throughout the study and the residence time was changed by varying the pyridine feed rate. The hydrogen flow rate, measured downstream of the reactor, was adjusted to obtain the required initial pyridine partial pressure.

The areas under different peaks on the chromatograms were

measured by triangulation. This method is reported[31] to have a precision of 4%.

The effect of the different variables viz. temperature, residence time, and initial pyridine partial pressure on the conversion was studied. Figures 4 through 7 show the variation of product distribution with temperature at initial pyridine partial pressures of 49.3, 91.8, 133.8, and 165.5 k Pa.

Legend for Figures 4-7:

⬡ Pyridine ○ Piperidine ▽ Pentylamine

△ Pentylpiperidine ◇ Ammonia ● Pentane

□ Unidentified N_2 Base

Figures 8 and 9 show the effect of P_{pyr_o} on the formation and disappearance by reaction of piperidine with temperature as a parameter.

The first step in pyridine hydrodenitrogenation viz. the formation of piperidine was chosen for kinetic studies. Figures 10, 11 and 12 are plots of conversion vs. time data for initial pyridine partial pressures of 106.0, 134.1 and 181.2 k Pa respectively with temperature as a parameter.

Experimental data was fitted to theoretical rate expressions by means of a least squares fit program utilizing an IBM 360 computer (Appendix F).

The reaction has been found to exhibit pseudo-zero order kinetics in that while the reaction rate is independent of the pyridine partial pressure during the course of the reaction, it was dependent on the initial pyridine partial pressure, C_{pyr_o}. Furthermore, the "order" of the reaction rate constant in C_{pyr_o} was found to vary with temperature as follows:

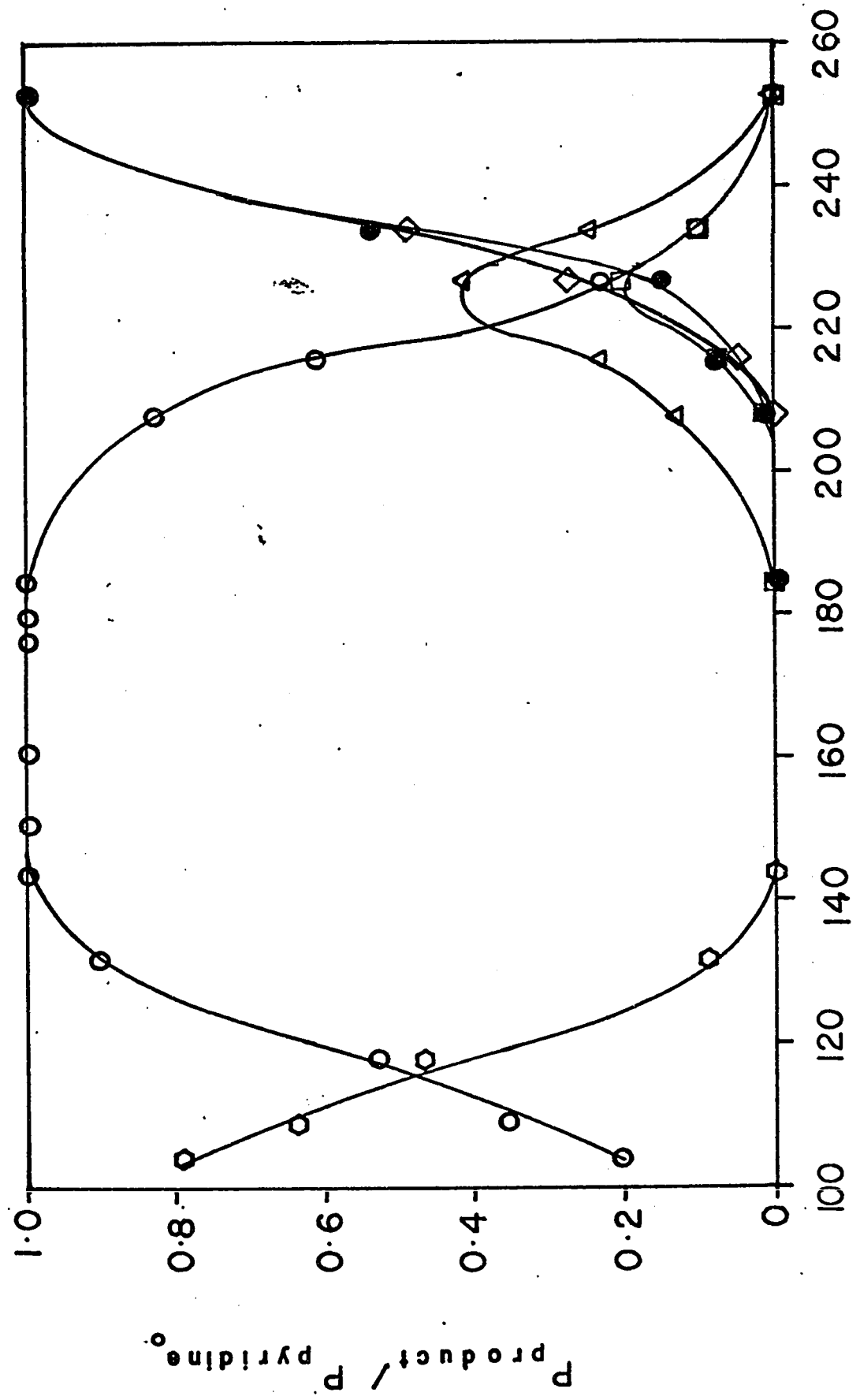

Fig. 4. Product distribution vs temperature. (P_{P_o} = 493 k Pa, P_f = 0.0261 moles/hr.)

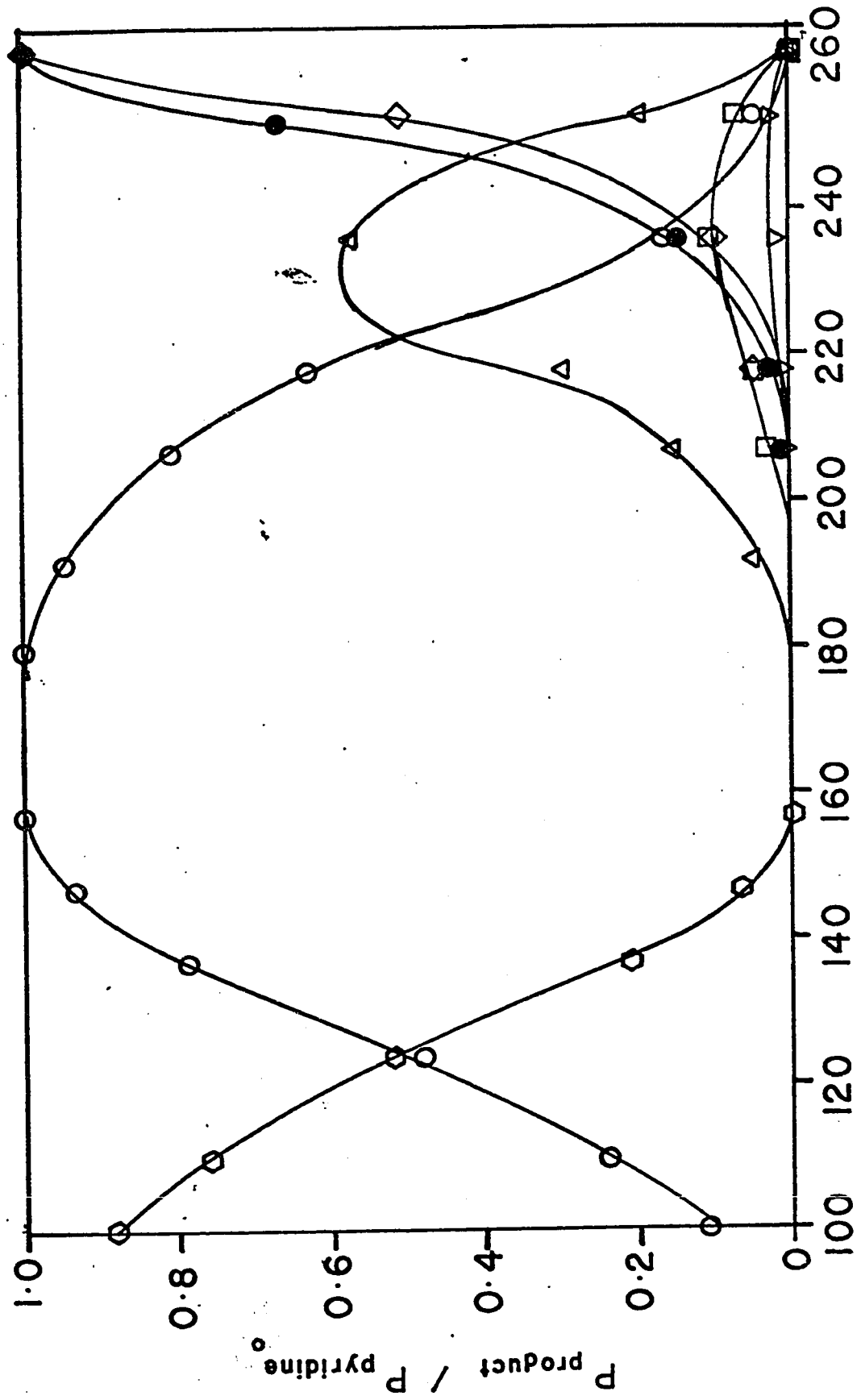

Fig. 5. Product distribution vs temperature. (P_{p_o} = 918 k Pa, P_f = 0.0490 moles/hr.)

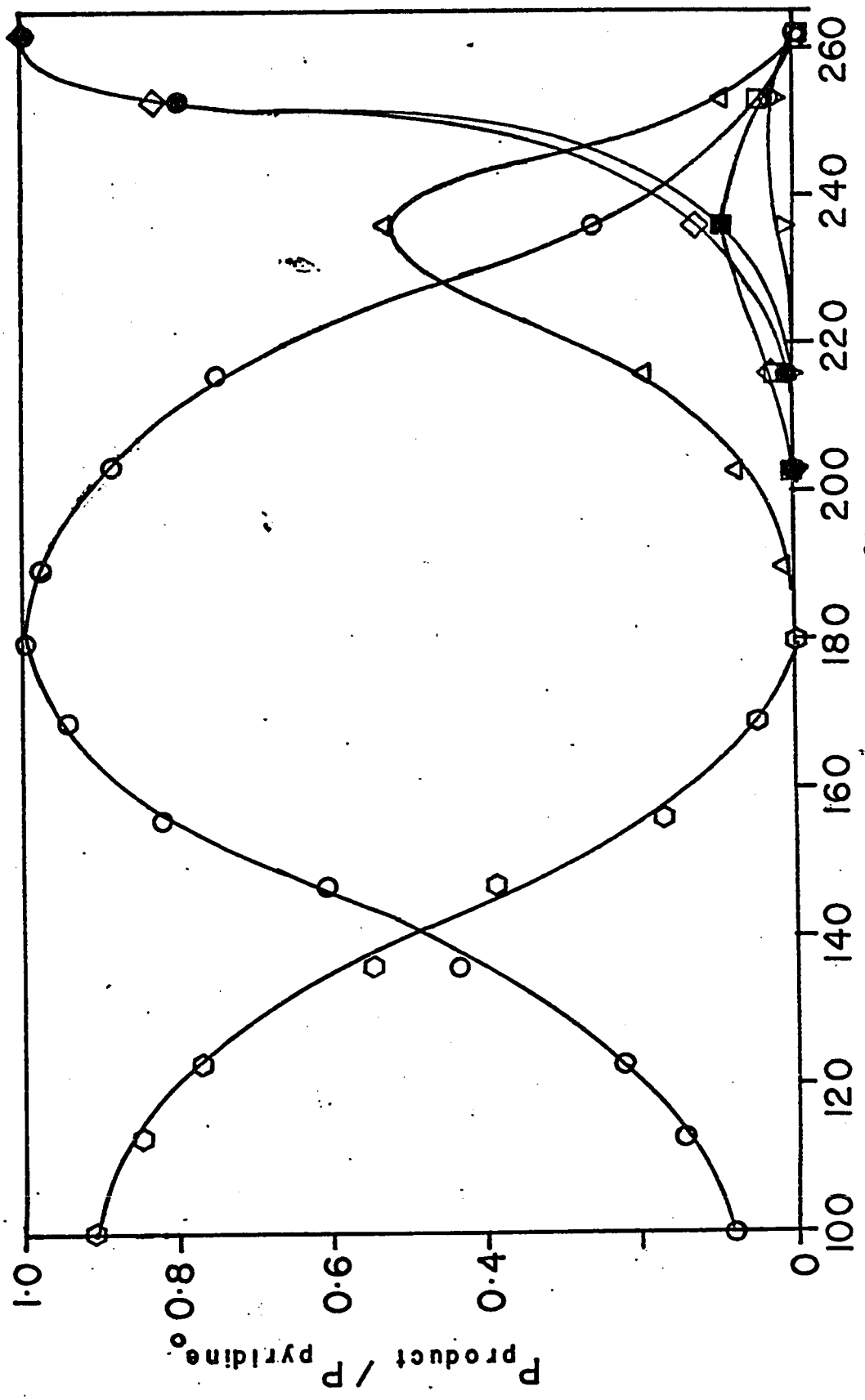

Fig. 6. Product distribution vs temperature. (P_{po} = 133.8 k Pa, P_f = 0.0721 moles/hr.)

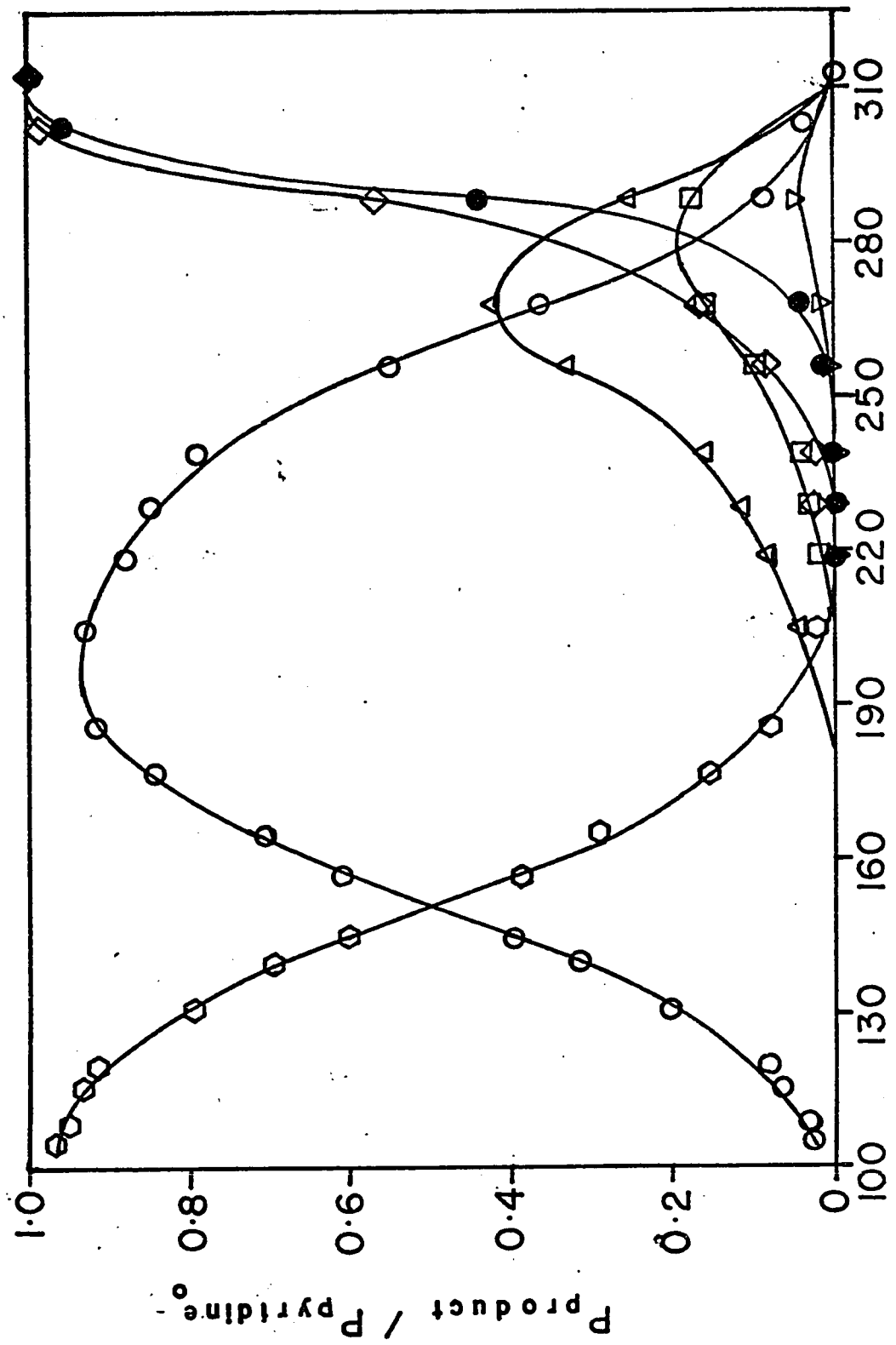

Fig. 7. Product distribution vs temperature. (P_{p_o} = 165.5 k Pa, P_f = 0.0969 moles/hr.)

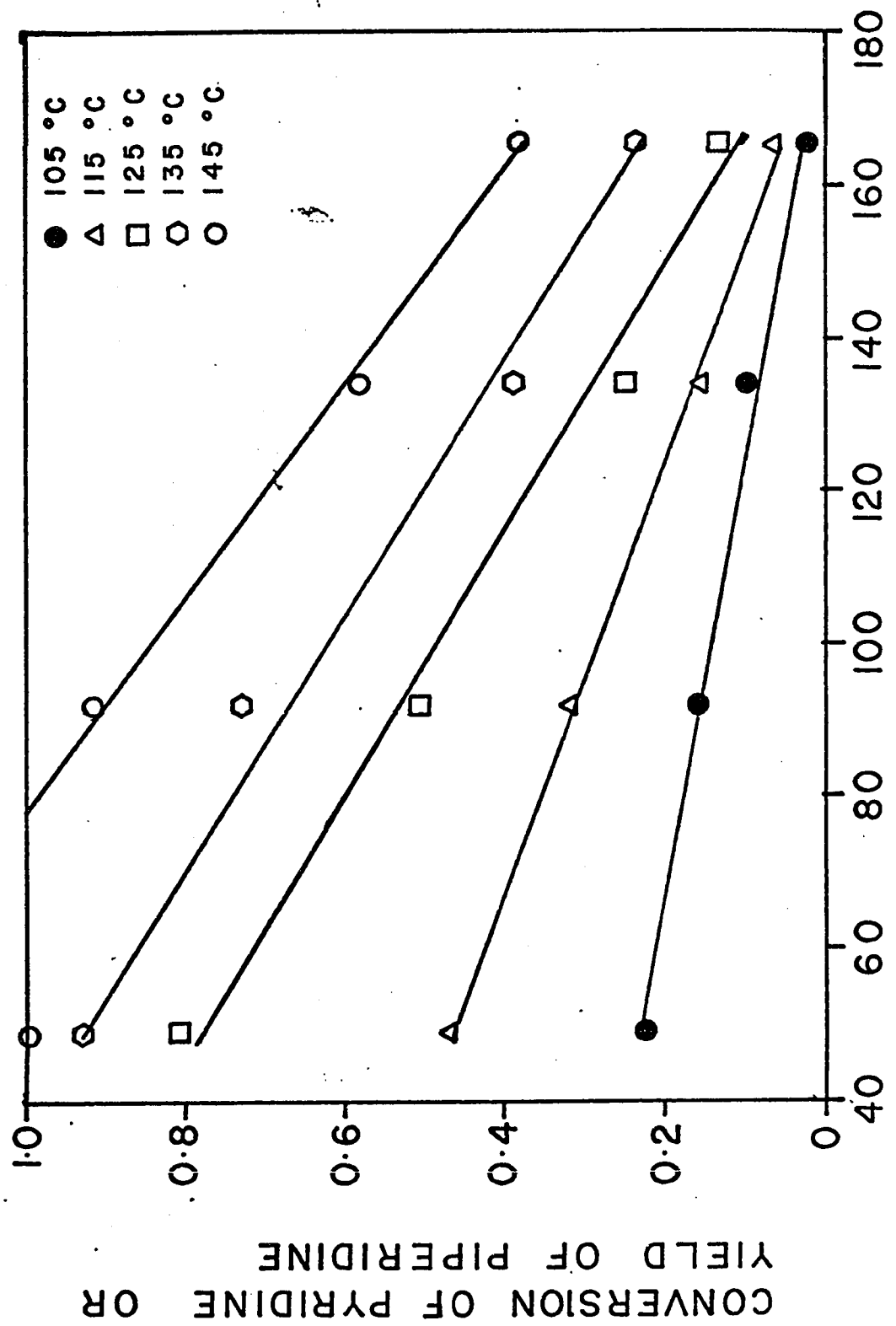

Fig. 8. Conversion of pyridine vs initial pyridine partial pressure.

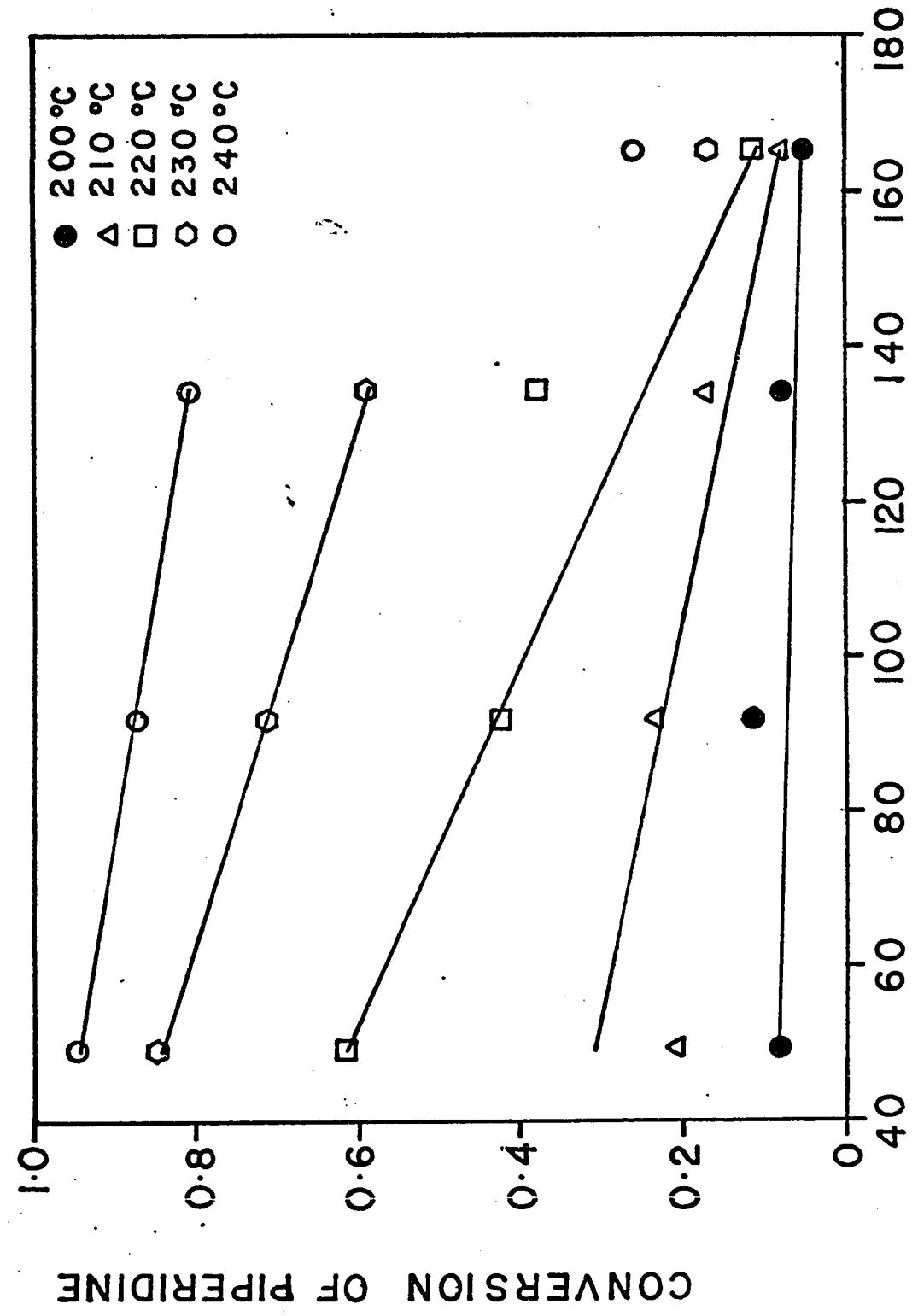

Fig. 9. Conversion of piperidine vs initial pyridine partial pressure.

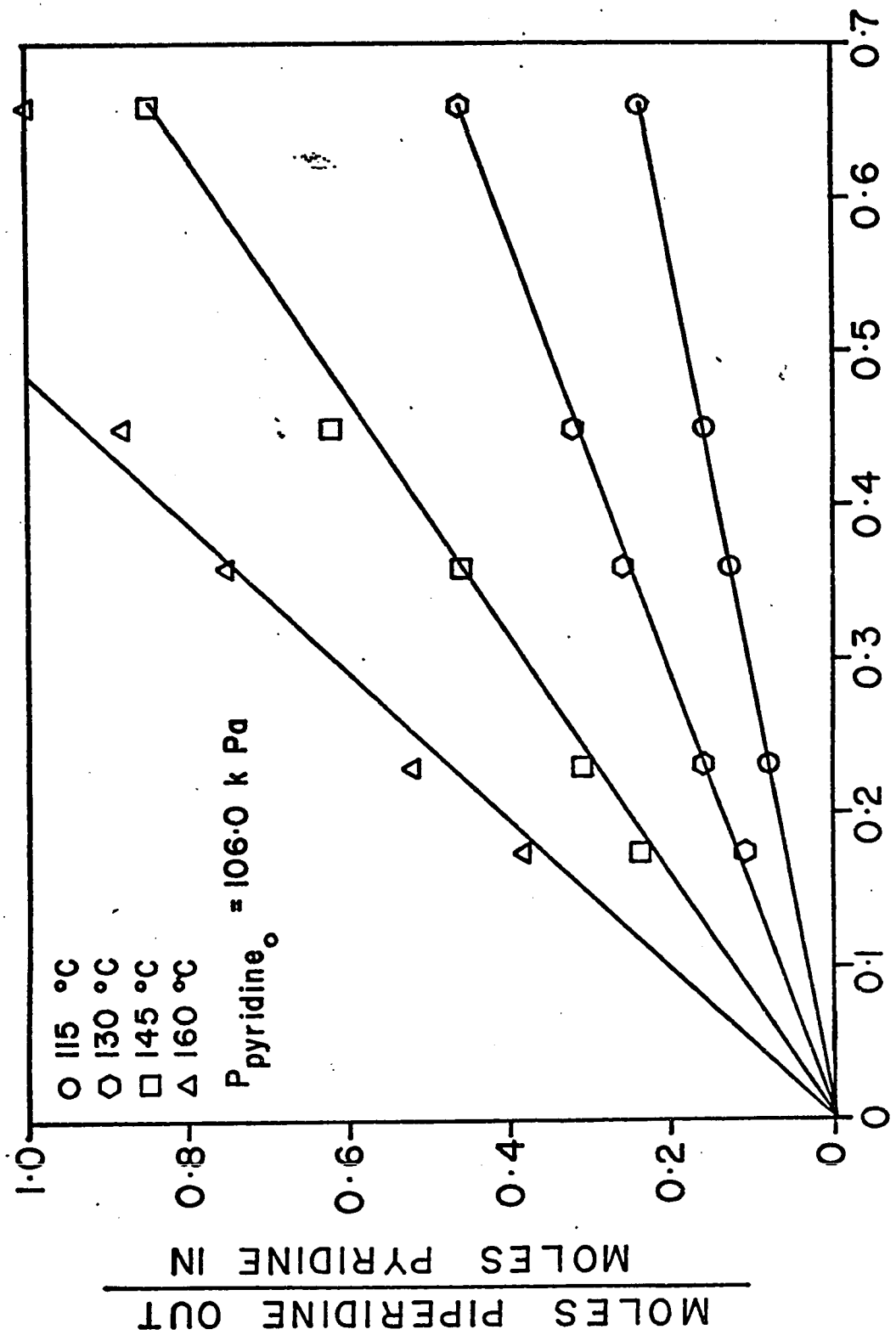

Fig. 10. Conversion vs residence time.

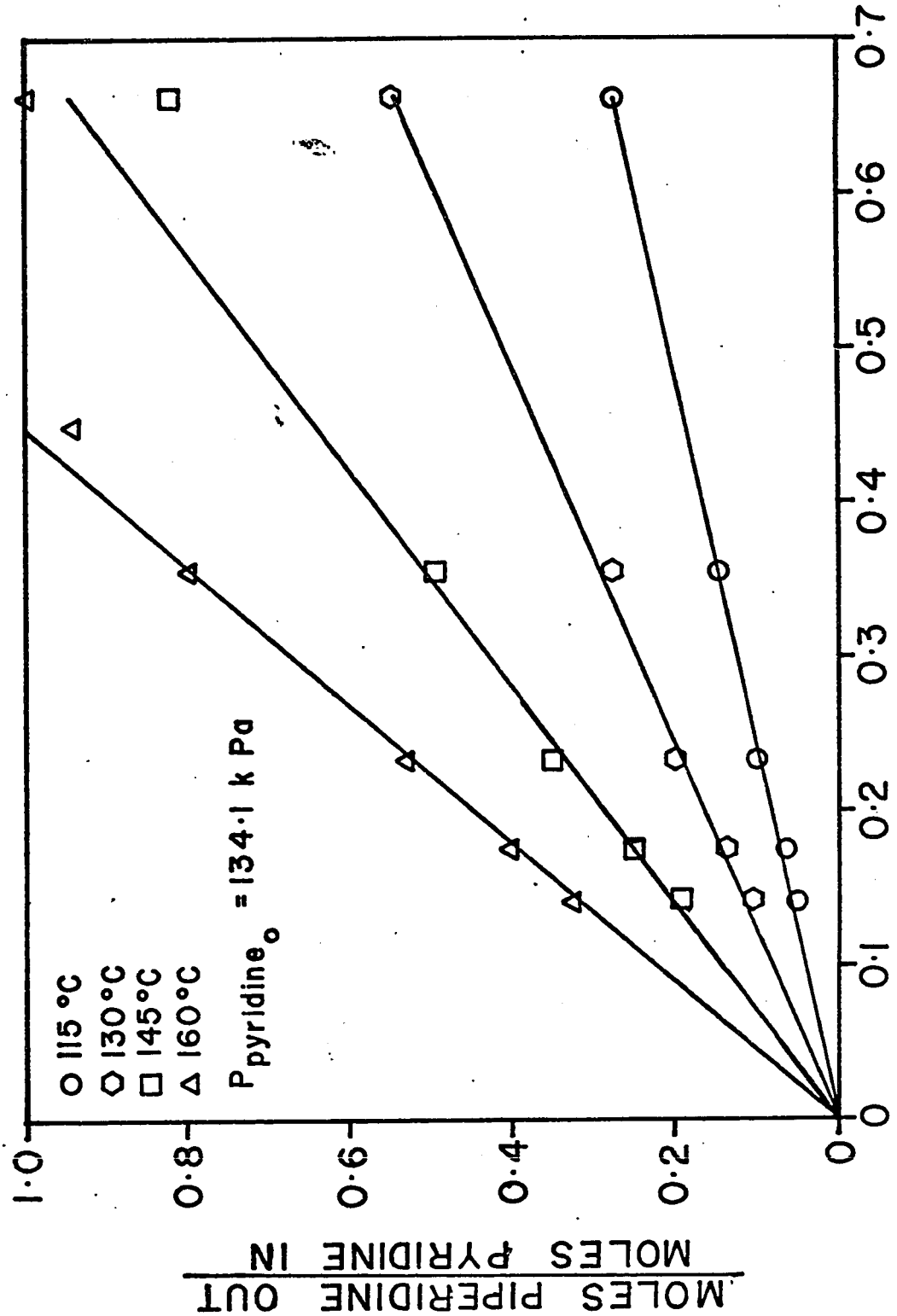

Fig. 11. Conversion vs residence time.

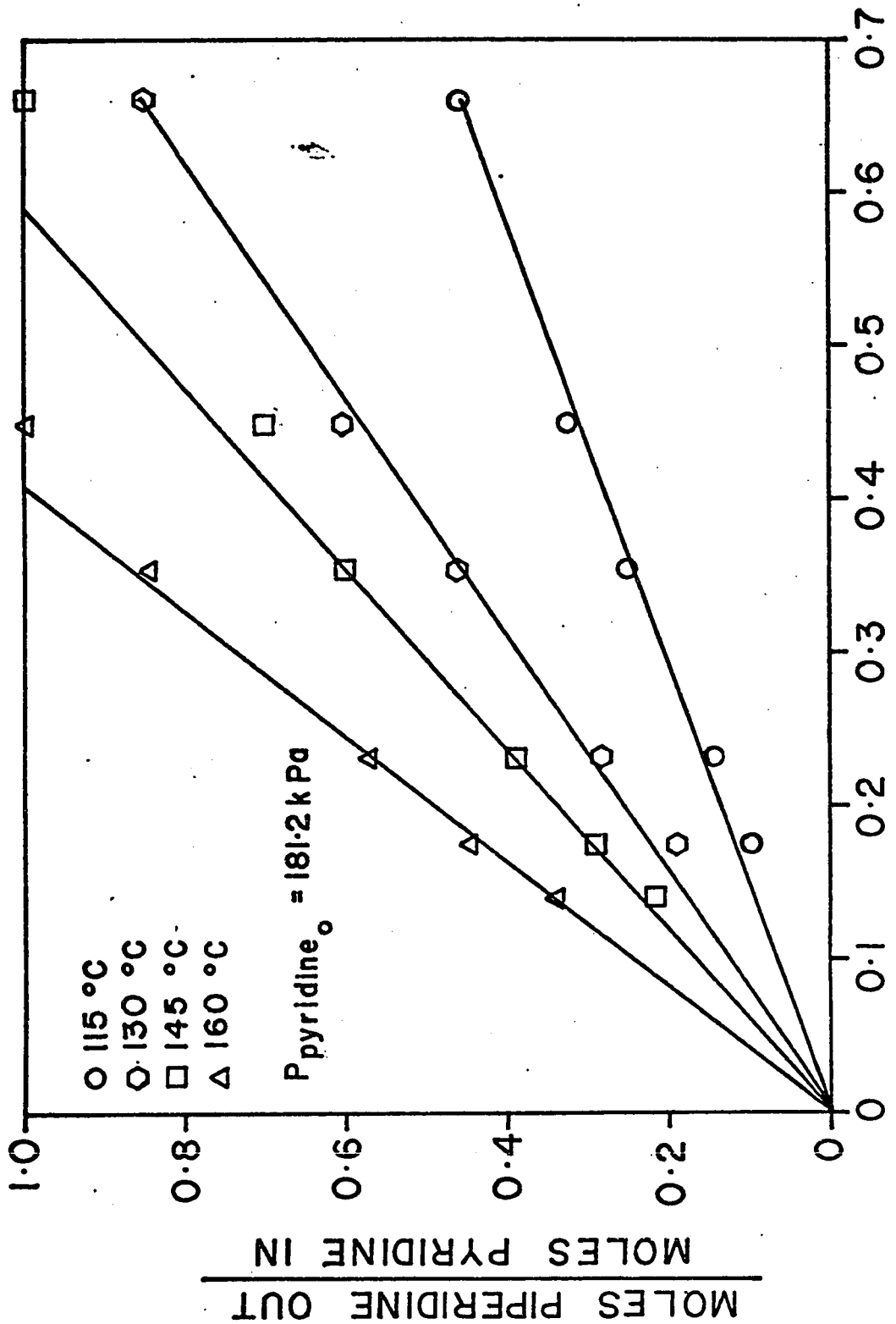

Fig. 12. Conversion vs residence time.

TEMPERATURE °C	ORDER IN C_{pyr_o}
115	2.23
130	2.15
145	1.50
160	1.30

The order in C_{H_o} was found to be zero over the concentration range studied.

Pseudo-second-order rate constants were calculated and the energy of activation was calculated to be 11.51 k cal. The pre-exponential factor was 2.48×10^7.

Figure 13 ($\ell n\ K_p$ vs $\frac{1}{T}$) shows the temperature-dependency of the pseudo-equilibrium constant. Thus, the rate expression is found to be

$$r = K_p\ (C_{pyr_o})^n$$

where K_p and n are temperature-dependent.

K_p can be expressed as:

$$\ell n\ K_p = 17.025 - \frac{11514}{RT}$$

and n can be expressed as

$$\ell n\ n = 33.050 - 5.40\ \ell n\ T$$

$$(388°K < T < 433°K)$$

Figure 14 shows the temperature-dependency of n.

Alternatively, the pseudo-zero-order rate constant, K, can be used to calculate the frequency factor and activation energy at different concentrations to get:

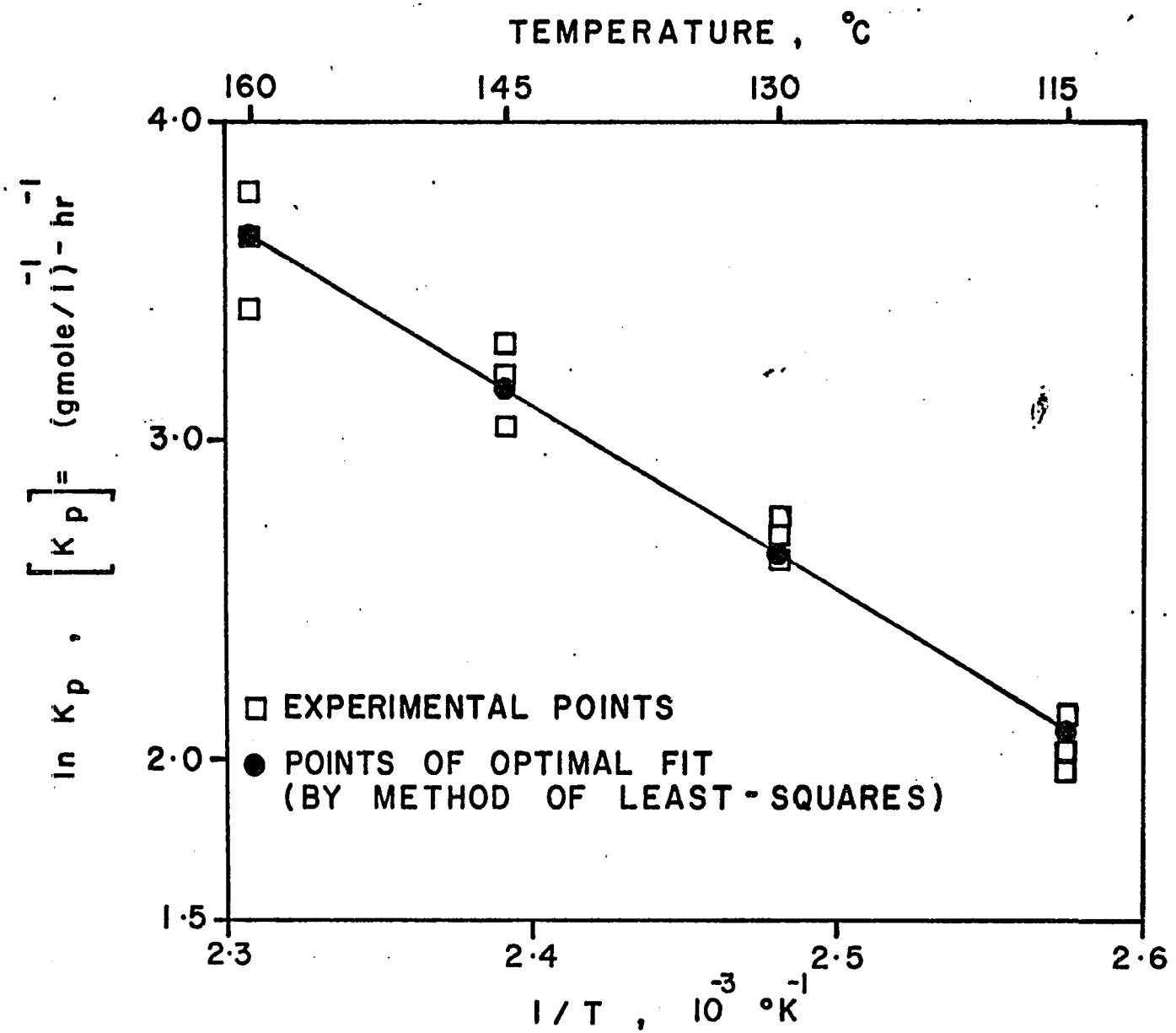

Fig. 13. Arrhenius plot for pseudo-second-order rate constant.

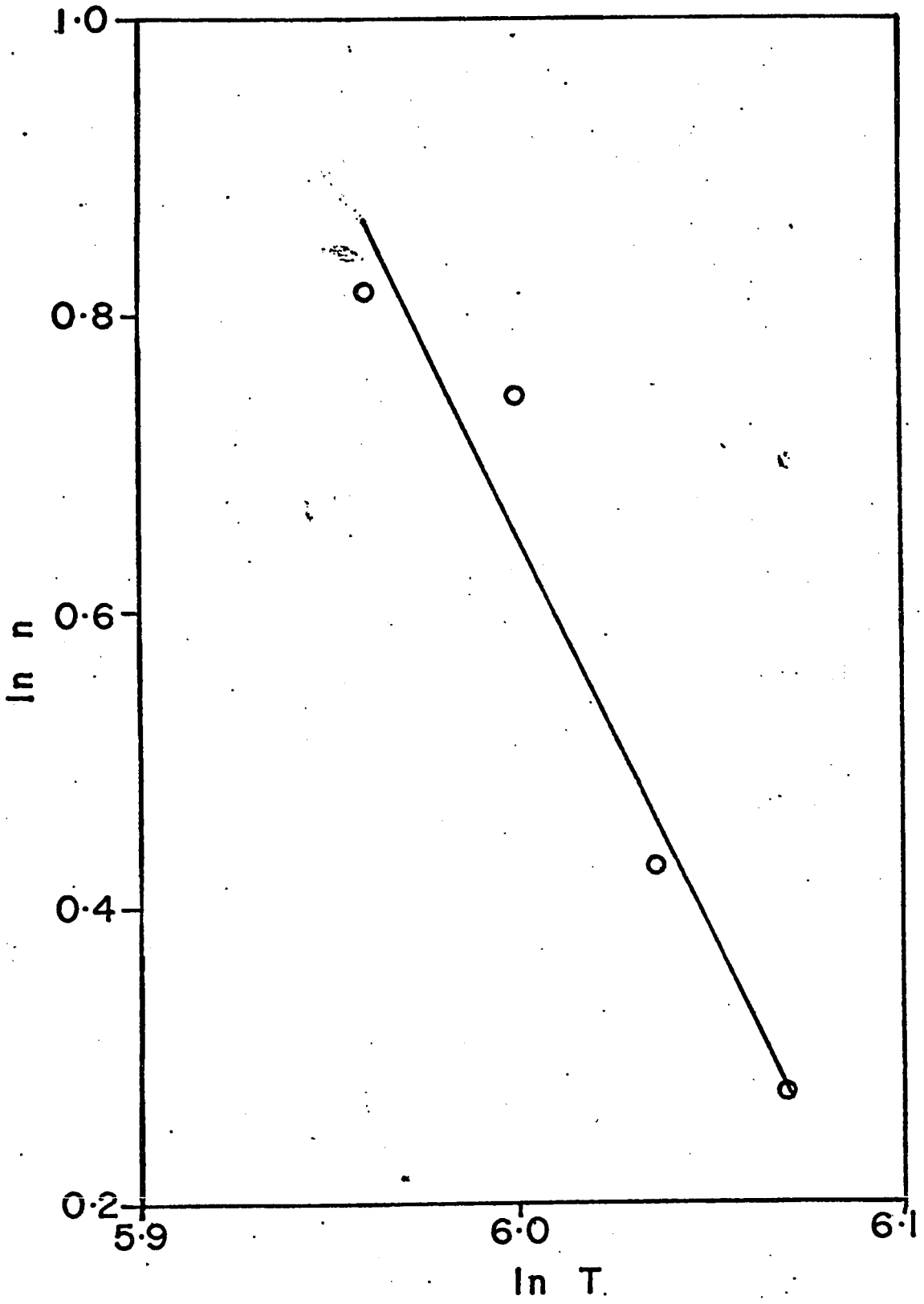

Fig. 14. Log_e n versus Log_e T.

$$\ell n\ K = 12.89 - \frac{13080}{RT} \qquad \text{for } P_{p_o} = 106.0 \text{ k Pa}$$

$$= 12.428 - \frac{12400}{RT} \qquad \text{for } P_{p_o} = 134.1 \text{ k Pa}$$

$$= 8.94 - \frac{9080}{RT} \qquad \text{for } P_{p_o} = 181.2 \text{ k Pa}$$

The temperature-dependency of this pseudo-rate constant is shown in Figure 15. Table 1 gives a summary of calculated results.

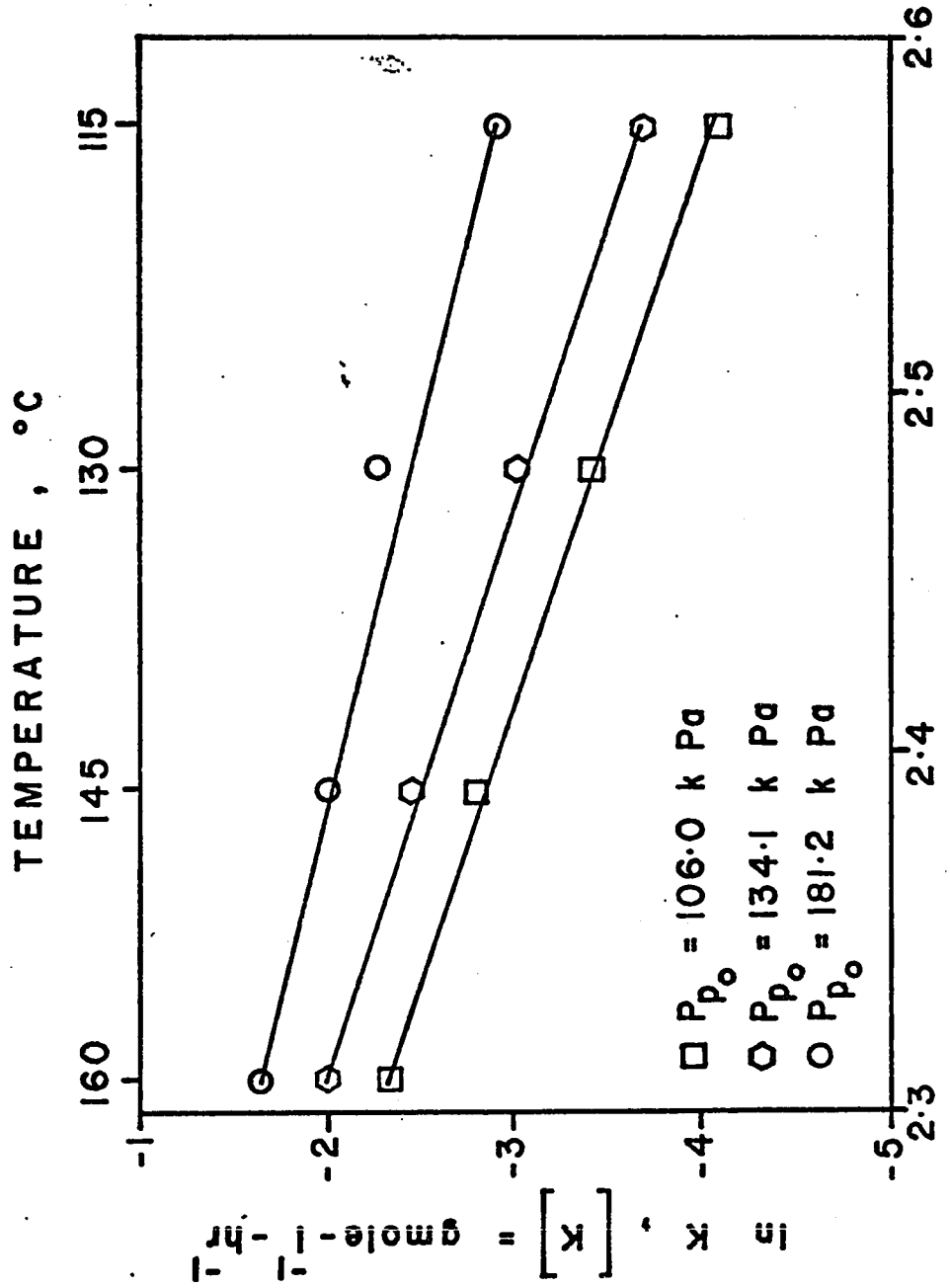

Fig. 15. Arrhenious plot for pseudo-zero-order rate constant.

Table 1. Summary of results.

T °C	P_{p_o} k Pa	C_{P_o} gmole-ℓ^{-1}	x/t hr^{-1}	r=K gmole-ℓ^{-1}-hr^{-1}	K_p (gmole-ℓ^{-1})$^{-1}$$hr^{-1}$	n	For K k_o	For K E_o k cal
115	106.0	4.6693×10^{-2}	0.3583	16.73×10^{-3}	7.67	2.23		
130	106.0	4.6693×10^{-2}	0.7000	32.68×10^{-3}	14.99	2.14	3.96×10^{5}	13.080
145	106.0	4.6693×10^{-2}	1.2833	59.92×10^{-3}	27.48	1.50		
160	106.0	4.6693×10^{-2}	2.0667	96.50×10^{-3}	44.26	1.30		
115	134.1	5.9062×10^{-2}	0.4250	25.10×10^{-3}	7.20	2.23		
130	134.1	5.9062×10^{-2}	0.8233	48.63×10^{-3}	13.94	2.14	2.50×10^{5}	12.400
145	134.1	5.9062×10^{-2}	1.4383	84.95×10^{-3}	24.35	1.50		
160	134.1	5.9062×10^{-2}	2.2500	132.89×10^{-3}	38.10	1.30		
115	181.2	7.9829×10^{-2}	0.6863	54.79×10^{-3}	8.60	2.23		
130	181.2	7.9829×10^{-2}	1.2833	102.45×10^{-3}	16.08	2.14	7.36×10^{3}	9.080
145	181.2	7.9829×10^{-2}	1.6800	134.11×10^{-3}	21.04	1.50		
160	181.2	7.9829×10^{-2}	2.4286	193.87×10^{-3}	30.42	1.30		

For K_p i.e. when n = 2,

$$\ell n\ K_p = 17.025 - \frac{11514}{RT}$$

CHAPTER 6

DISCUSSION

There are four significant aspects of the results of this investigation:

(i) The HDN of pyridine takes place in two distinct steps - hydrogenation of pyridine to piperidine and the subsequent conversion of piperidine to pentane and ammonia via pentylamine, pentylpiperidine and dipentylamine.

(ii) The pyridine hydrogenation reaction shows zero-order behaviour i.e.

$$r = K$$

(iii) The zero-order reaction rate constant, K, varies with temperature and the initial pyridine concentration, C_{p_o}, such that

$$K = K_p \ (C_{p_o})^n$$

where K_p is a pseudo rate constant dependent only on temperature, and n is the order in initial pyridine concentration, decreasing with temperature (2.23 at 115°C and 1.30 at 160°C).

(iv) Alternatively, the activation energy calculated for pseudo-zero-order kinetics decreases with starting pyridine partial pressure (13.08 k cal at 106.0 k Pa and 9.08 k cal at 186.2 k Pa).

While a reaction scheme of the form

$$\text{Pyridine} + H_2 \longrightarrow \text{Piperidine}$$

$$\text{Piperidine} + H_2 \longrightarrow \text{Consecutive products}$$

has been proposed for some time now, this study shows conclusively that

the reaction does indeed take place in two distinct and independent steps viz. the formation of piperidine and the subsequent conversion of piperidine to pentane and ammonia via pentylamine, dipentylamine, and pentylpiperidine. Under the reaction conditions employed, the first step was found to go to completion and pyridine did not play any role in the second step.

The zero-order kinetics exhibited by the reaction suggests that the rate-controlling step in the reaction mechanism is either adsorption of pyridine or desorption of piperidine. This supposition is corroborated by using the approach of Yang and Hougen[30]. Figure 2, a plot of initial rate vs initial pyridine partial pressure, indicates that the reaction is controlled by the adsorption of pyridine. These results therefore imply that pyridine is strongly adsorbed, while hydrogen is either weakly adsorbed or possibly reacts from a van der Walls layer of physically adsorbed hydrogen. This, in effect, amounts to a non-equilibrium adsorption mechanism, known as the Rideal-Eley mechanism.

Some other hydrogenation reactions have been found to exhibit zero-order kinetics. Farkas et al[33] and Amano et al[34] have reported similar behaviour for benzene hydrogenation. Thomas and Thomas[32] have discussed these reactions from a theoretical standpoint and have explained this behaviour satisfactorily assuming the operation of a Rideal-Eley mechanism.

The variation of the zero-order rate constant with concentration indicates the operation of a Langmuir-Hinshelwood mechanism which assumes that the rate is controlled by reaction of adsorbed pyridine and adsorbed hydrogen and that all adsorption-desorption processes are in equilibrium.

The Rideal-Eley mechanism suggested by the zero-order kinetics and the Langmuir-Hinshelwood mechanism suggested by the variation in the zero-order rate constant with concentration can therefore be said to be operating simultaneously. The extent to which either mechanism influences the reaction rate would depend on the temperature and initial pyridine concentration. The Langmuir-Hinshelwood mechanism would also account for the change in the order of the reaction.

Bond and Newham[35] studied the hydrogenation of cyclopropane over metal catalysts. The order with respect to cyclopropane was found to increase with temperature at constant hydrogen pressure. This behaviour was explained[32] on the basis of a Langmuir-Hinshelwood mechanism.

The variation in the activation energy (calculated for the pseudo-zero-order rate constant) with the initial pyridine partial pressure could be due to the fact that the observed activation energy would vary with the heat of adsorption, which itself is a function of coverage. Coverage may be defined as the fraction of the active surface that is covered by pyridine. At higher initial pyridine concentrations, a larger fraction of the surface is covered by pyridine resulting in increased heat of adsorption. This would tend to decrease the observed value of the activation energy.

The coverage would also depend on the temperature - it would decrease with an increase in temperature. This would affect the order of the reaction and would account, at least partially, for the change in the order of the reaction with temperature.

The results of this investigation differ considerably from published data. Sonnemans et al[5-9] have not reported the activation energy for the formation of piperidine. However, it can be estimated

from their data[5] and was found to be of the order of 41 k cal. The thermodynamic data calculated by Satterfield et al[13] shows that the activation energy for the uncatalyzed homogeneous reaction should approximate 47 k cal. This shows that Sonnemans' study of the catalyzed reaction, in fact, approached the uncatalyzed reaction. This was possibly due to the very poor activity shown by their catalyst as compared to the activity of the catalyst used in this study (the possible reasons for the difference in activity are discussed later). Chegolya et al[16] studied the liquid-phase hydrogenation of pyridine over alumina-supported ruthenium catalysts and reported an activation energy of 15-16 k cal. This value is comparable to the value estimated in this study (11.5 k cal) though the seemingly large difference (35%) is due to the different catalysts and due to the fact that they studied the reaction in the liquid phase.

The reaction has been reported to be pseudo-first-order in pyridine[1,4,7] while in this study pseudo-zero-order kinetics were observed. This could happen, if in this study, the rate-controlling step was different from that in the other investigations. A Langmuir-Hinshelwood model was used to fit the data obtained in the other investigations, suggesting thereby that surface-reaction was the rate-controlling step. A Rideal-Eley mechanism is indicated in this study showing that adsorption rather than surface reaction is the rate-determining step. In other words, the surface reaction was found to be very fast and essentially at equilibrium while adsorption was relatively slower and hence removed from equilibrium. This, again, could be due to the vast difference in the catalytic activity between this study and the other investigations.

Sonnemans et al calculated the reaction rate using a residence time based on the total number of moles fed to the reactor. This residence time incorporates the effect of concentration and would show up in the concentration-dependence of the rate constant and in the order of the reaction. On the other hand, a residence time based on the limiting reactant only (used in this investigation) is independent of concentration and will give more representative results.

The catalyst used by Sonnemans et al[6-9] was basically similar to the 'Harshaw' catalyst used in this study in that both were alumina-supported cobalt-molybdate catalysts. However, their catalyst had been obtained from Ketjen, Amsterdam. A sample of an alumina-supported cobalt-molybdate catalyst obtained from Ketjen - known hereinafter as the Ketjen catalyst - and a sample of the Harshaw catalyst were subjected to a comparative spectrographic analysis. Four major differences were observed. The Ketjen catalyst contained large amounts of silica and sodium while the Harshaw catalyst was almost free of these impurities. Further, the Harshaw catalyst contained 3-5 times the amount of nickel and titanium present in the Ketjen catalyst. The extremely high activity of nickel in hydrogenation reactions was thought to have improved the activity of the Harshaw catalyst while the silica and sodium in the Ketjen catalyst could have reduced its activity. Moreover, Sonnemans et al activated their catalyst for only 16 hours while, in this study, the catalyst was activated for 48 hours. One batch of catalyst was activated for 16 hours only and the activity was found to be much lower than the activity of a conditional batch of catalyst which had been activated for 48 hours.

Also, Sonnemans et al had to operate at relatively higher temperatures because of the poor activity of their catalyst. As seen from Figure 3, the equilibrium of the pyridine-hydrogen-piperidine system starts moving towards pyridine at high temperatures. Thus, they were operating at conditions very close to equilibrium and were dealing with a reversible reaction while the high catalytic activity enabled this study to be performed at much lower temperatures where the reaction is practically irreversible. This was another reason why surface reaction was found to be very fast compared to the adsorption of pyridine.

The extremely low concentration of pentylamine and the identifiable - but unmeasurable - amounts of dipentylamine in the reaction products indicate the reaction scheme shown on the following page.

In order to account for the very low concentrations of pentylamine and dipentylamine in the product stream, reactions 1, 3, 4 and 7 would have to be much faster than the others and so have been depicted as irreversible.

The order in hydrogen could not be estimated because a vast excess of hydrogen was required to prevent condensation in the reactor and, as such, the hydrogen concentration could be varied to a very limited extent.

1. 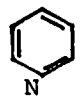 + 3 H_2 ⟶ 

Pyridine — Piperidine

2.  + H_2 ⇌ $C_5H_{11}-NH_2$

Piperidine — Pentylamine

3. $C_5H_{11}-NH_2$ + H_2 ⟶ C_5H_{12} + NH_3

Pentylamine — Pentane Ammonia

4. $C_5H_{11}-NH_2$ + 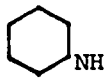 ⟶  + NH_3

Pentylamine — Piperidine — Pentylpiperidine — Ammonia

5. 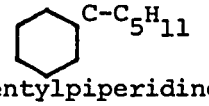 + H_2 ⇌  + C_5H_{12}

Pentylpiperidine — Piperidine — Pentane

6. $2C_5H_{11}-NH_2$ ⇌ $C_5H_{11}-NH-C_5H_{11}$ + NH_3

Pentylamine — Dipentylamine — Ammonia

7. $C_5H_{11}-NH-C_5H_{11}$ + H_2 ⟶ $C_5H_{11}-NH_2$ + C_5H_{12}

Dipentylamine — Pentylamine — Pentane

CHAPTER 7

RECOMMENDATIONS

The following recommendations are made with regard to pursuance of this study:

a) Because of the extreme sensitivity of the reaction rate to temperature, a very rigid control over the ambient temperature is required.

b) The effect of varying the total pressure should be studied next. This would also permit investigation of the order of the reaction in hydrogen. Since higher flow rates might be needed to stay out of the bulk diffusion-controlled region, it would be judicious to set up an apparatus capable of handling larger throughputs. Otherwise, the pressure-drop across the reactor and the tubing might become significant.

c) The final phase of the project would be to study the kinetics of the HDN of pyridine dissolved in "clean" crude oil. This study could be carried out on at least a semi-pilot-plant scale.

CHAPTER 8

NOMENCLATURE

a:	activity of reactants
a_m:	surface area of catalyst, sq.cm./gm.
A_l, A_r:	area under the peak on the chromatogram for components l and r
C_p:	molal specific heat
C_{pyr}:	concentration of pyridine, gmole/ℓ
e:	base to natural logarithms
E:	effectiveness factor
E_o:	activation energy, k cal
f_l:	relative weight factor for component l
F:	feed rate of pyridine vapour at reactor pressure, cu.cm./hr.
G_M:	molal mass velocity based on total cross-sectional area of bed, gmole/hr-sq.cm.
ΔH_R:	heat of reaction, k cal/gmole
k_o:	pre-exponential factor
k_n:	piperidine denitrification rate constant
k_{pyr}:	reaction velocity constant for pyridine
K:	reaction rate constant
K_A, K_N:	adsorption coefficients for ammonia and piperidine
K_e:	overall equilibrium constant
K_p:	pseudo rate constant
K_{pyr}:	adsorption equilibrium constant for pyridine
L:	total number of active sites
m:	exponent for adsorption term

n: order of the reaction

p_f: pyridine feed rate, moles/hr.

P_A, P_H, P_N: partial pressures of ammonia, hydrogen and piperidine

P_{pyr_o}: initial pyridine partial pressure, k Pa

P_t: total pressure, M Pa

ΔP: pressure drop, Pa

r: reaction rate, gmole/ℓ-hr

r_j: molal reaction rate of component j per unit mass of catalyst

r_o: initial reaction rate, gmole/ℓ-hr.

R: universal gas constant, cal/gmole-°K

t: space time, hr.

T: absolute temperature, °K

ΔT: temperature difference, °C

W: volume of the catalyst, cu.cm.

W_l, W_r: weight fractions of components l and r

x: fractional conversion

$y_{j_{in}}, y_{j_{out}}$: mole fraction of component j in reactants and products

y_{pyr}: average mole fraction of pyridine

ϕ: shape factor for catalyst particles

Subscripts

A: ammonia

f: final

H: hydrogen

j: component j

N: piperidine

o: initial

p,pyr: pyridine

pip: piperidine

P: pseudo

Abbreviations

AMM: ammonia

HDN: hydrodenitrogenation

PF: pyridine feed rate, gmoles/hr.

PE-AM: pentylamine

PE-PIP: pentylpiperidine

PENT: pentane

PIP: piperidine

PPO: initial pyridine partial pressure

PRODUCT COMPOSITION: moles of product out per mole of pyridine feed

PRODUCT RATE: product flow rate, gmole/hr

PYR: pyridine

TEMP: temperature

UNID: unidentified nitrogen base

CHAPTER 9

BIBLIOGRAPHY

1. Cox, K.E., Ph.D. Thesis, Montana State College, Bozeman, Montana, 1961.

2. Somers, A.E., unpublished data (1965). Through McIlvried[4].

3. Rosenheimer, M.O., Kiovsky, J.R., Preprints, Vol. 12, No. 4, p. B-147, Division of Petroleum Chemistry, 154th Meeting, ACS, Chicago, Ill., September 1967.

4. McIlvried, H.G., Ind. Eng. Chem. Proc. Des. Develop., 10, 125 (1971).

5. Sonnemans, J., Goudriaan, F., Mars, P., Catal. Proc. Int. Congr., 5th, 1972 (published 1973), (2), 1085.

6. Sonnemans, J., Mars, P., J. Catal., 31, 209 (1973).

7. Sonnemans, J., Van Den Berg, G.H., Mars, P., ibid, 31, 220 (1973).

8. Sonnemans, J., Mars, P., ibid, 34, 215 (1974).

9. Sonnemans, J., Neyens, W.J., Mars, P., ibid, 34, 230 (1974).

10. Satterfield, C.N., Modell, M., Mayer, J.F., AI.Ch.E.J., 21, 1100 (1975).

11. Satterfield, C.N., Modell, M., Mayer, J.F., Cocchetto, J.F., U.S.N.T.I.S., P.B. Rep. 1975, PB-248101. Through CA, 85, 82653g (1976).

12. Satterfield, C.N., Cocchetto, J.F., A.I.Ch.E.J., 21, 1107 (1975).

13. Cocchetto, J.F., Satterfield, C.N., Ind. Eng. Chem. Proc. Des. Develop., 15, 272 (1976).

14. Baltz, H., Smeykall, K., Moll, K.K., Bruesehaber, L., Britain 1,109,640 (Cl. C07d), 10 April 1968, Appl. 28 March 1967. Through CA, 69, 52009d (1968).

15. Katzer, J.R., Gates, B.C., Olson, J.H., Kwart, H., Stiles, A.B., Report 1975, FE-2028-1, avail. N.T.I.S. Through CA, 86, 75694p (1977).

16. Chegolya, A.S., Mikhailov, G.D., Malykh, V.A., Karakhanov, R.A., Shuikin, N.I., Izv. Akad. Nauk SSSR, Ser. Khim., 3, 682 (1968). Through CA, 69, 70178n (1968).

17. Dyukareva, V.N., Tr. Molodykh Uch., Saratov. Univ., Vyp. Khim., 2,162 (1971). Through CA, 79, 78544f (1973).

18. Smeykal, K., Moll, K.K., Chem. Tech. (Berlin), 19(2), 92 (1967). Through CA, 66, 104878w (1967).

19. Sultanov, A.S., Khasanov, A.K., Safaev, A.S., Abidov, B.V., Katal. Pererab. Uglevodorodn. Syr'ya, 1, 68 (1967). Through CA, 71, 12967z (1969).

20. Sultanov, A.S., Safaev, A.S., Khasanov, A.K., Abidov, B.A., Akhundzhanov, A.I., ibid, 2, 39(1968). Through CA, 71, 101672s (1969).

21. Safaev, A.S., Akhundzhanov, A.I., Sultanov, A.S., ibid, 4, 101 (1970). Through CA, 76, 59400c (1972).

22. Safaev, A.S., Faiziev, T.F., Bagdasarova, I.A., Tr. Tashk. Politekh. Inst., 90, 49 (1972). Through CA, 83, 193019h (1975).

23. Safaev, A.S., Bagdasarova, I.A., Mukhitdinov, R., ibid, 107, 61 (1973). Through CA, 82, 170628w (1975).

24. Yasui, H., Echi, H., Japan 68 14,467 (Cl. 16E431.1) 19 June 1968, Appl. 25 May 1965. Through CA, 70, 77796s (1969).

25. Madkour, M.M., Mahmoud, B.H., Abdou, I.K., Vlutger, J.C., J. Indian Chem. Society, 46 (8), 720 (1969). Through CA, 71, 112775d (1969).

26. Beugeling, M., Boduszynski, M., Goudriaan, F., Sonnemans, J., Analytical Letters, 4, 727 (1971).

27. Dietz, W.A., J. Gas Chromatog., 5, 68 (1967).

28. Smith, J.M., "Chemical Engineering Kinetics", McGraw Hill, 2nd Edition (1970).

29. Yoshida, F., Ramaswami, D., Hougen, O.A., A.I.Ch.E.J., 8 (1), 5 (1962).

30. Yang, K.H., Hougen, O.A., Chemical Engineering Progress, 46(3), 146 (1950).

31. McNair, H.M., Bonelli, E.J., "Basic Gas Chromatography", Gow Mac Instrument Company.

32. Thomas, J.M., Thomas, W.J., "Introduction to the Principles of Heterogeneous Catalysis", Academic Press (1967).

33. Farkas, A., Farkas, L., Trans. Faraday Soc., 33, 927 (1937).

34. Amano, A., Parravno, G., Adv. Catalysis, 9, 716 (1957).

35. Bond, G.C., Newham, J., Trans. Faraday Soc., 56, 1851 (1960).

APPENDIX A

CALIBRATION

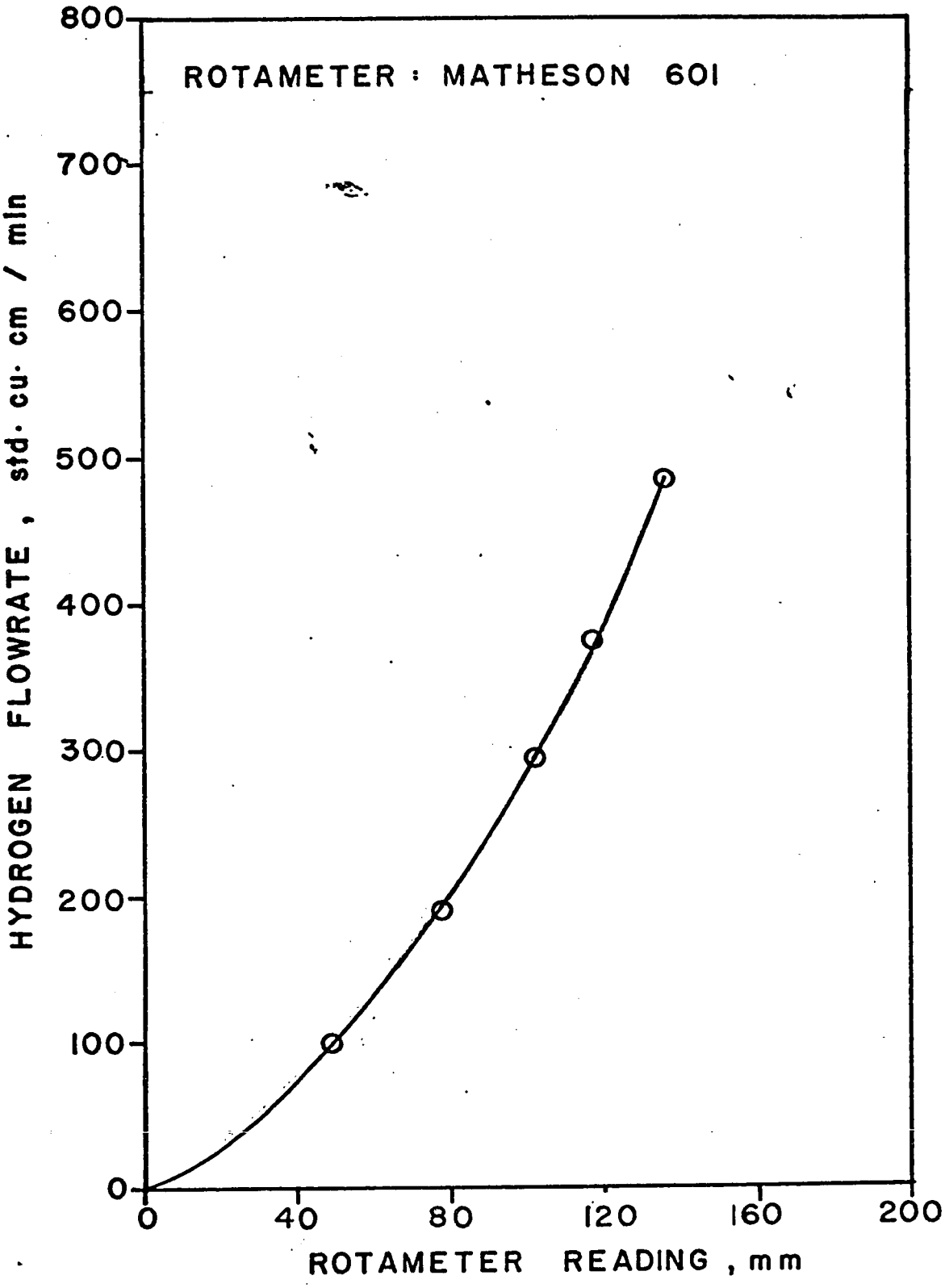

Fig. 16. Calibration curve for rotameter.

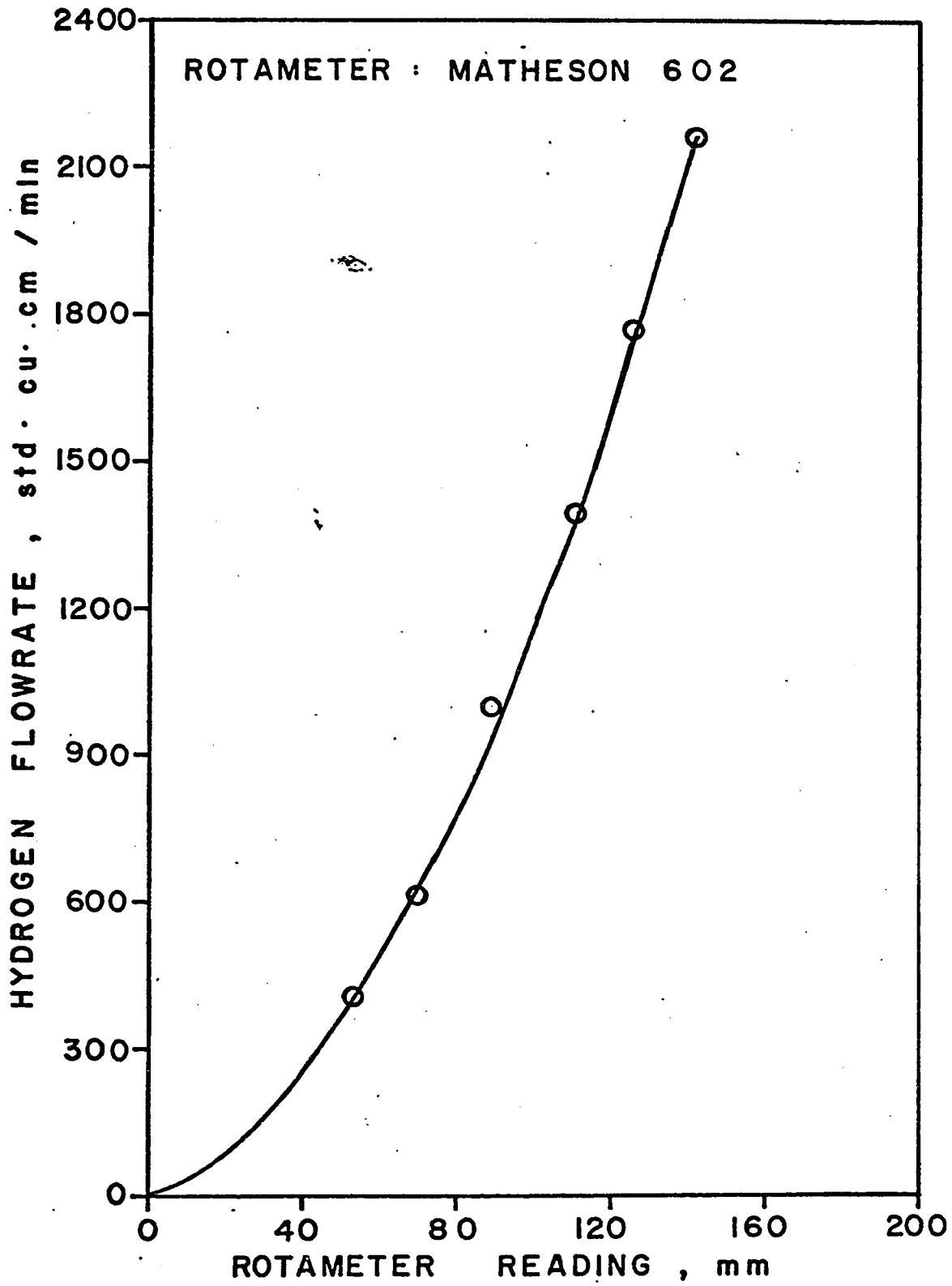

Fig. 17. Calibration curve for rotameter.

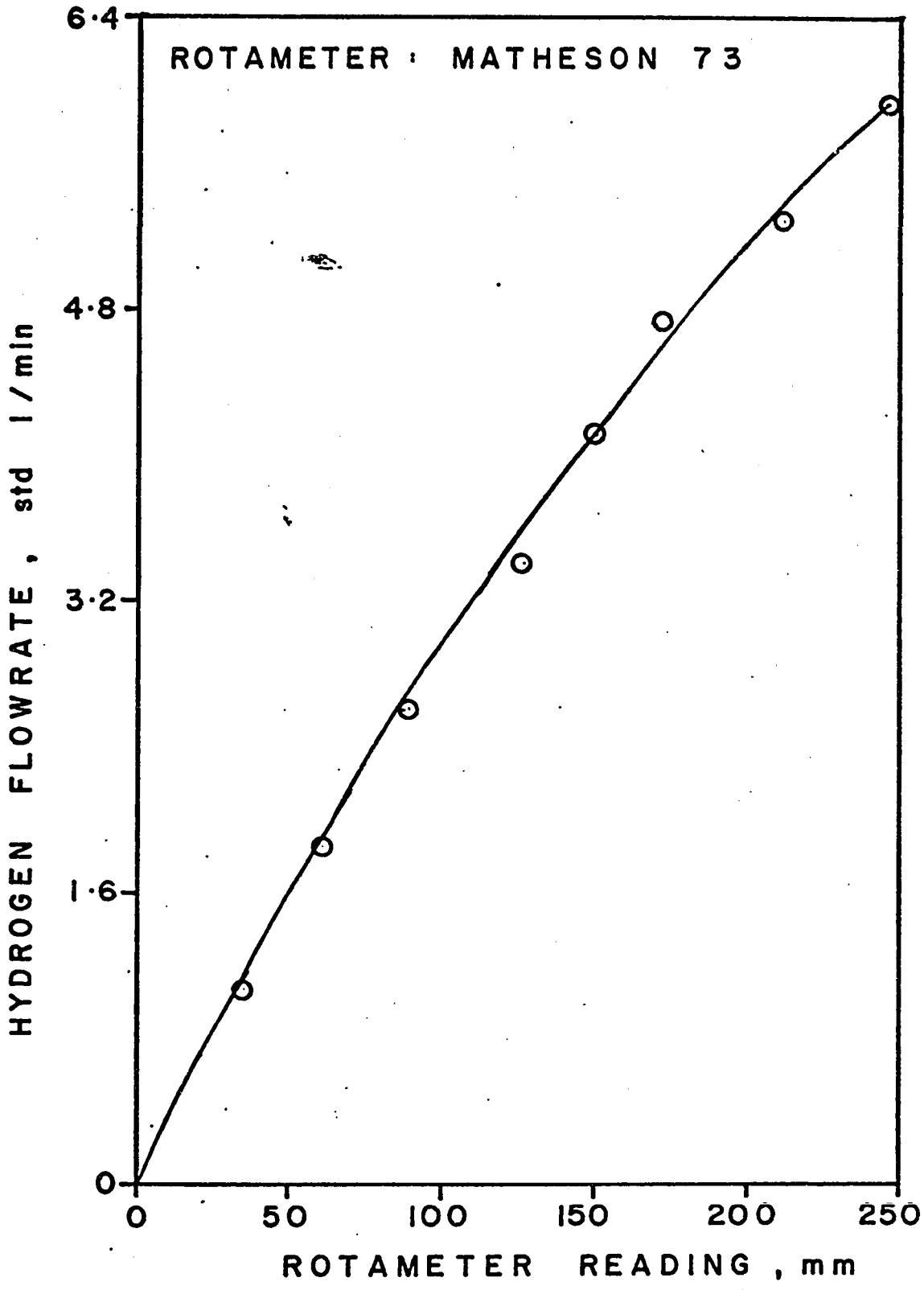

Fig. 18. Calibration curve for rotameter.

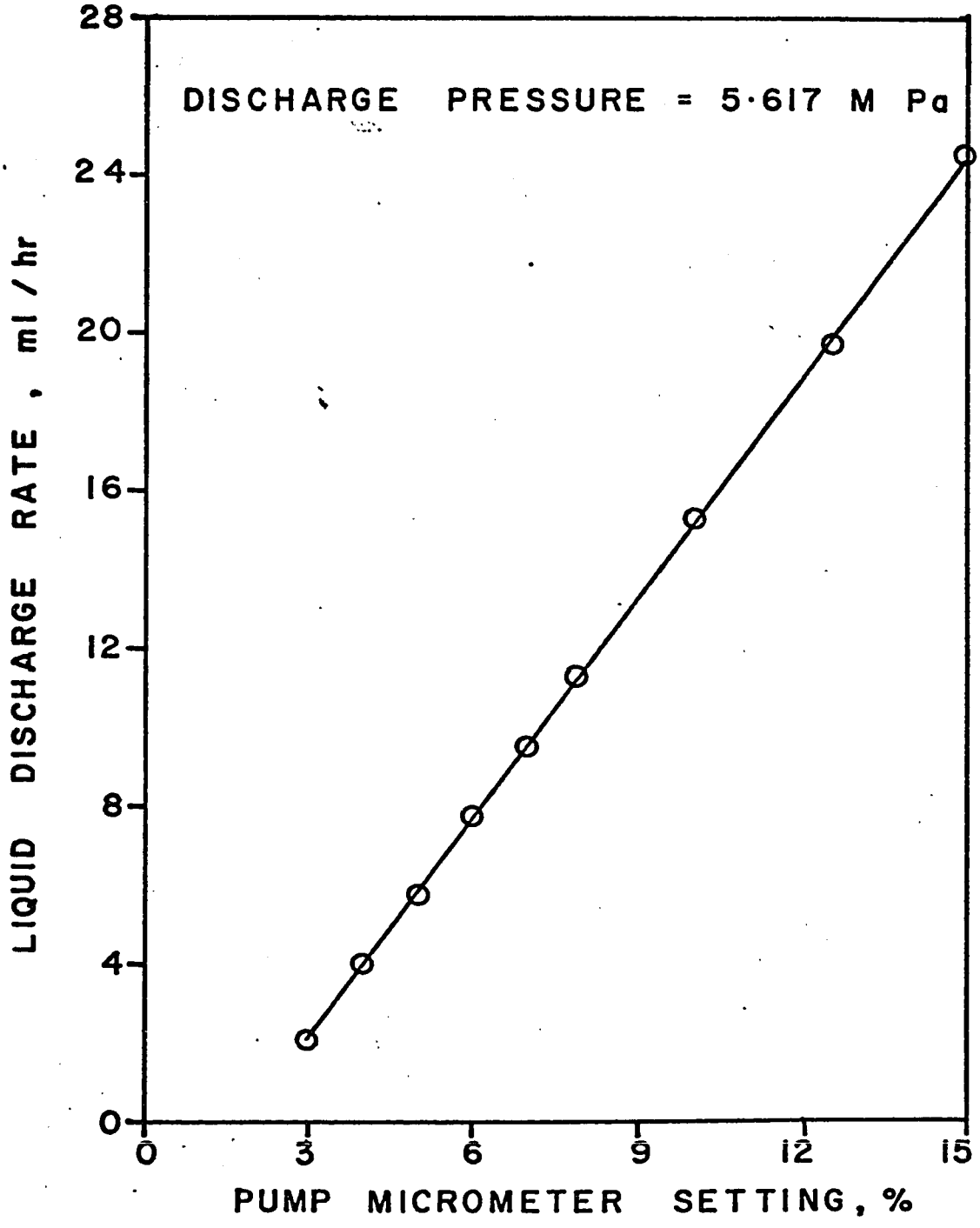

Fig. 19. Calibration curve for liquid minipump.

Mixtures containing varying, but known, amounts of pyridine, piperidine, pentylamine, and pentane were prepared and samples injected into the chromatograph. The areas under the peaks for each component were measured by triangulation.

Relative weight factor was defined as:

$$f_1 = \left(\frac{W_1}{W_r}\right) \Big/ \left(\frac{A_1}{A_r}\right)$$

where

f_1 is the relative weight factor of component 1 with respect to component r,

W_1 and W_r are weight fractions of components 1 respectively

A_1 and A_r are areas under the peaks for components 1 and r respectively, corrected for the change of instrument sensitivity if any.

Piperidine was chosen as the reference component. Relative weight factors for the components were calculated over a wide range of compositions and averaged. Their values are as below:

COMPONENT	RELATIVE WEIGHT FACTOR
Pyridine	0.9438
Piperidine	1.0000
Pentane	0.8274
Pentylamine	0.6801

The value of the relative weight factor for piperidine has been reported[15] as 0.83. Weight factors for the different compounds relative to a weight factor of 0.83 for piperidine can be found by multiplying the relative weight factors obtained by 0.83 to get the following values:

COMPONENT	WEIGHT FACTOR
Pyridine	0.7834 ≃ 0.78
Piperidine	0.8300 ≃ 0.83
Pentane	0.6867 ≃ 0.69
Pentylamine	0.5645 ≃ 0.56

The weight factors for ammonia and pentylpiperidine could not be measured and were taken from literature:

COMPONENT	WEIGHT FACTOR
Ammonia	0.42[15]
Pentylpiperidine	0.92[14]

These weight factors were used to calculate the product composition. The molecular weights were used to convert the mass fractions into mole fractions.

The unidentified nitrogen base was assumed to have a weight factor and a molecular weight equal to that for piperidine.

APPENDIX B

EXPERIMENTAL DATA

All the readings were taken at a total pressure of 5.617 M Pa. The catalyst quantity was kept constant at 10.365 gm throughout the experiment.

The following symbols are used:

PPO: initial pyridine partial pressure

PF: pyridine feed rate, moles per hour

Product Rate: moles of product out per hour

Product Composition: moles of product out per mole of pyridine feed

Pyr: pyridine

Pip: piperidine

Pe-am: pentylamine

Pe-pip: pentylpiperidine

Amm: ammonia

Pent: pentane

Unid: unidentified nitrogen base

RUN NO.	PPO, K PA	PF, MOLES/HR	TEMP, DEG C	PRODUCT RATE		PRODUCT COMPOSITION	
				PYR	PIP	PYR	PIP
101	49.3	0.0261	104	0.0204	0.0053	0.794	0.206
102	49.3	0.0261	109	0.0168	0.0094	0.641	0.359
103	49.3	0.0261	118	0.0129	0.0143	0.474	0.526
104	49.3	0.0261	132	0.0025	0.0241	0.095	0.905
105	49.3	0.0261	144	0.0000	0.0253	0.000	1.000
106	49.3	0.0261	151	0.0000	0.0256	0.000	1.000
107	49.3	0.0261	161	0.0000	0.0266	0.000	1.000
108	49.3	0.0261	177	0.0000	0.0257	0.000	1.000
109	49.3	0.0261	180	0.0000	0.0263	0.000	1.000
110	49.3	0.0261	185	0.0000	0.0261	0.000	1.000
116	91.8	0.0490	100	0.0423	0.0056	0.884	0.116
117	91.8	0.0490	110	0.0374	0.0120	0.757	0.243
118	91.8	0.0490	124	0.0260	0.0241	0.519	0.481
119	91.8	0.0490	137	0.0101	0.0383	0.209	0.791
120	91.8	0.0490	147	0.0032	0.0496	0.065	0.935
121	91.8	0.0490	157	0.0000	0.0477	0.000	1.000
122	91.8	0.0490	180	0.0000	0.0498	0.000	1.000
129	133.8	0.0721	100	0.0650	0.0059	0.917	0.083
130	133.8	0.0721	113	0.0623	0.0108	0.852	0.148
131	133.8	0.0721	123	0.0551	0.0160	0.775	0.225
132	133.8	0.0721	136	0.0384	0.0316	0.549	0.451
133	133.8	0.0721	147	0.0276	0.0434	0.389	0.611
134	133.8	0.0721	156	0.0125	0.0587	0.176	0.824

RUN NO.	PPO, K PA	PF, MOLES/HR	TEMP, DEG C	PRODUCT RATE		PRODUCT COMPOSITION	
				PYR	PIP	PYR	PIP
135	133.8	0.0721	169	0.0040	0.0674	0.056	0.944
136	133.8	0.0721	180	0.0000	0.0726	0.000	1.000
143	165.5	0.0969	104	0.0877	0.0027	0.970	0.030
144	165.5	0.0969	109	0.0848	0.0032	0.964	0.036
145	165.5	0.0969	116	0.0834	0.0057	0.936	0.064
146	165.5	0.0969	120	0.0835	0.0075	0.918	0.082
147	165.5	0.0969	131	0.0696	0.0177	0.797	0.203
148	165.5	0.0969	140	0.0613	0.0280	0.687	0.313
149	165.5	0.0969	145	0.0529	0.0348	0.603	0.397
150	165.5	0.0969	157	0.0341	0.0532	0.391	0.609
151	165.5	0.0969	165	0.0268	0.0649	0.292	0.708
152	165.5	0.0969	177	0.0136	0.0753	0.153	0.847
153	165.5	0.0969	186	0.0072	0.0833	0.080	0.920
163	106.0	0.0124	115	0.0094	0.0029	0.763	0.237
164	106.0	0.0721	115	0.0614	0.0114	0.844	0.156
165	106.0	0.0915	115	0.0789	0.0113	0.875	0.125
166	106.0	0.1394	115	0.1263	0.0117	0.915	0.085
167	106.0	0.0124	130	0.0068	0.0058	0.538	0.462
168	106.0	0.0721	130	0.0485	0.0227	0.682	0.318
169	106.0	0.0915	130	0.0672	0.0237	0.739	0.261
170	106.0	0.1394	130	0.1199	0.0228	0.840	0.160
171	106.0	0.1845	130	0.1613	0.0193	0.893	0.107
172	106.0	0.0124	145	0.0019	0.0104	0.154	0.846

RUN NO.	PPO, K PA	PF, MOLES/HR	TEMP, DEG C	PRODUCT RATE		PRODUCT COMPOSITION	
				PYR	PIP	PYR	PIP
173	106.0	0.0721	145	0.0274	0.0454	0.376	0.624
174	106.0	0.0915	145	0.0489	0.0415	0.541	0.459
175	106.0	0.1394	145	0.0976	0.0445	0.687	0.313
176	106.0	0.1845	145	0.1395	0.0431	0.764	0.236
177	106.0	0.0124	160	0.0000	0.0127	0.000	1.000
178	106.0	0.0721	160	0.0083	0.0627	0.117	0.883
179	106.0	0.0915	160	0.0235	0.0695	0.253	0.747
180	106.0	0.1394	160	0.0671	0.0733	0.478	0.522
181	106.0	0.1845	160	0.1125	0.0698	0.617	0.383
182	134.1	0.0124	115	0.0088	0.0033	0.725	0.275
183	134.1	0.0915	115	0.0789	0.0135	0.854	0.146
184	134.1	0.1394	115	0.1243	0.0138	0.900	0.100
185	134.1	0.1845	115	0.1708	0.0188	0.935	0.065
186	134.1	0.2298	115	0.2209	0.0126	0.946	0.054
187	134.1	0.0124	130	0.0060	0.0069	0.462	0.538
188	134.1	0.0915	130	0.0645	0.0246	0.724	0.276
189	134.1	0.1394	130	0.1177	0.0276	0.810	0.190
190	134.1	0.1845	130	0.1554	0.0247	0.863	0.137
191	134.1	0.2298	130	0.2011	0.0241	0.893	0.107
192	134.1	0.0124	145	0.0023	0.0104	0.180	0.820
193	134.1	0.0915	145	0.0450	0.0443	0.504	0.496
194	134.1	0.1394	145	0.0932	0.0502	0.650	0.350
195	134.1	0.1845	145	0.1369	0.0456	0.750	0.250

RUN NO.	PPO, K PA	PF, MOLES/HR	TEMP, DEG C	PRODUCT RATE		PRODUCT COMPOSITION	
				PYR	PIP	PYR	PIP
196	134.1	0.2298	145	0.1864	0.0446	0.807	0.193
197	134.1	0.0124	160	0.0000	0.0119	0.000	1.000
198	134.1	0.0721	160	0.0042	0.0689	0.058	0.942
199	134.1	0.0915	160	0.0188	0.0725	0.206	0.794
200	134.1	0.1394	160	0.0651	0.0732	0.471	0.529
201	134.1	0.1845	160	0.1146	0.0754	0.603	0.397
202	134.1	0.2298	160	0.1543	0.0742	0.676	0.325
203	181.2	0.0124	115	0.0069	0.0059	0.538	0.462
204	181.2	0.0721	115	0.0475	0.0230	0.674	0.326
205	181.2	0.0915	115	0.0691	0.0233	0.748	0.252
206	181.2	0.1394	115	0.1213	0.0206	0.855	0.145
207	181.2	0.1845	115	0.1604	0.0182	0.898	0.102
208	181.2	0.0124	130	0.0018	0.0106	0.145	0.855
209	181.2	0.0721	130	0.0294	0.0448	0.396	0.604
210	181.2	0.0915	130	0.0414	0.0482	0.462	0.538
211	181.2	0.1394	130	0.0985	0.0396	0.713	0.287
212	181.2	0.1845	130	0.1521	0.0361	0.808	0.192
213	181.2	0.0124	145	0.0000	0.0123	0.000	1.000
214	181.2	0.0721	145	0.0217	0.0514	0.297	0.703
215	181.2	0.0915	145	0.0049	0.0074	0.397	0.603
216	181.2	0.1394	145	0.0869	0.0558	0.609	0.391
217	181.2	0.1845	145	0.1288	0.0531	0.708	0.292
218	181.2	0.2298	145	0.1863	0.0522	0.781	0.219

RUN NO.	PPO, K PA	PF, MOLES/HR	TEMP, DEG C	PRODUCT RATE		PRODUCT COMPOSITION	
				PYR	PIP	PYR	PIP
219	181.2	0.0721	160	0.0000	0.0712	0.000	1.000
220	181.2	0.0915	160	0.0143	0.0786	0.154	0.846
221	181.2	0.1394	160	0.0577	0.0775	0.427	0.573
222	181.2	0.1845	160	0.1053	0.0844	0.555	0.445
223	181.2	0.2298	160	0.1539	0.0789	0.661	0.339

RUN NO.	PPO K PA	PF MOLES/HR	TEMP DEG C	PRODUCT RATE				
				PYR	PIP	PE-AM	PE-PIP	PENT
111	49.3	0.0261	208	0.0000	0.0210	0.0000	0.0034	0.0004
112	49.3	0.0261	216	0.0000	0.0164	0.0000	0.0061	0.0022
113	49.3	0.0261	227	0.0000	0.0060	0.0000	0.0109	0.0039
114	49.3	0.0261	234	0.0000	0.0027	0.0000	0.0064	0.0141
115	49.3	0.0261	253	0.0000	0.0000	0.0000	0.0000	0.0260
123	91.8	0.0490	192	0.0000	0.0469	0.0000	0.0025	0.0000
124	91.8	0.0490	207	0.0000	0.0387	0.0001	0.0072	0.0006
125	91.8	0.0490	218	0.0000	0.0304	0.0003	0.0142	0.0013
126	91.8	0.0490	236	0.0000	0.0081	0.0008	0.0283	0.0072
127	91.8	0.0490	253	0.0000	0.0022	0.0011	0.0095	0.0327
128	91.8	0.0490	262	0.0000	0.0000	0.0000	0.0000	0.0481
137	133.8	0.0721	190	0.0000	0.0688	0.0000	0.0015	0.0000
138	133.8	0.0721	203	0.0000	0.0658	0.0001	0.0058	0.0004
139	133.8	0.0721	216	0.0000	0.0538	0.0006	0.0140	0.0010
140	133.8	0.0721	236	0.0000	0.0186	0.0010	0.0378	0.0068
141	133.8	0.0721	253	0.0000	0.0026	0.0018	0.0071	0.0590
142	133.8	0.0721	262	0.0000	0.0000	0.0000	0.0000	0.0721
154	165.5	0.0969	205	0.0018	0.0826	0.0000	0.0042	0.0000
155	165.5	0.0969	219	0.0000	0.0807	0.0005	0.0079	0.0005
156	165.5	0.0969	229	0.0000	0.0743	0.0004	0.0101	0.0004
157	165.5	0.0969	239	0.0000	0.0714	0.0004	0.0146	0.0005
158	165.5	0.0969	256	0.0000	0.0493	0.0008	0.0295	0.0013
159	165.5	0.0969	268	0.0000	0.0320	0.0011	0.0371	0.0037

... continued

RUN NO.	PRODUCT RATE		PRODUCT COMPOSITION						
	AMM	UNID	PYR	PIP	PE-AM	PE-PIP	PENT	AMM	UNID
111	0.0000	0.0004	0.000	0.831	0.000	0.136	0.016	0.000	0.017
112	0.0015	0.0022	0.000	0.610	0.000	0.228	0.080	0.053	0.081
113	0.0077	0.0054	0.000	0.230	0.000	0.416	0.150	0.277	0.204
114	0.0129	0.0027	0.000	0.104	0.000	0.248	0.544	0.493	0.104
115	0.0260	0.0000	0.000	0.000	0.000	0.000	1.000	1.000	0.000
123	0.0000	0.0000	0.000	0.949	0.000	0.051	0.000	0.000	0.000
124	0.0000	0.0015	0.000	0.805	0.003	0.150	0.012	0.000	0.031
125	0.0022	0.0024	0.000	0.625	0.007	0.292	0.027	0.047	0.049
126	0.0047	0.0051	0.000	0.163	0.016	0.572	0.146	0.100	0.103
127	0.0249	0.0036	0.000	0.044	0.022	0.193	0.667	0.505	0.073
128	0.0496	0.0000	0.000	0.000	0.000	0.000	1.000	1.000	0.000
137	0.0000	0.0000	0.000	0.978	0.000	0.022	0.000	0.000	0.000
138	0.0007	0.0008	0.000	0.900	0.002	0.081	0.006	0.009	0.011
139	0.0023	0.0021	0.000	0.751	0.009	0.196	0.014	0.035	0.030
140	0.0094	0.0071	0.000	0.261	0.014	0.531	0.095	0.129	0.100
141	0.0609	0.0036	0.000	0.035	0.024	0.096	0.796	0.831	0.049
142	0.0728	0.0000	0.000	0.000	0.000	0.000	1.000	1.000	0.000
154	0.0000	0.0000	0.020	0.933	0.000	0.047	0.000	0.000	0.000
155	0.0000	0.0017	0.000	0.883	0.006	0.086	0.006	0.000	0.019
156	0.0024	0.0025	0.000	0.848	0.004	0.115	0.005	0.026	0.028
157	0.0024	0.0035	0.000	0.791	0.040	0.162	0.005	0.027	0.039
158	0.0078	0.0087	0.000	0.550	0.009	0.329	0.014	0.087	0.097
159	0.0148	0.0143	0.000	0.363	0.013	0.420	0.042	0.168	0.162

RUN NO.	PPO K PA	PF MOLES/HR	TEMP DEG C	PRODUCT RATE				
				PYR	PIP	PE-AM	PE-PIP	PENT
160	165.5	0.0969	288	0.0000	0.0074	0.0040	0.0217	0.0387
161	165.5	0.0969	303	0.0000	0.0035	0.0000	0.0000	0.0868
162	165.5	0.0969	313	0.0000	0.0000	0.0000	0.0000	0.0896

... continued

RUN NO.	PRODUCT RATE		PRODUCT COMPOSITION						
	AMM	UNID	PYR	PIP	PE-AM	PE-PIP	PENT	AMM	UNID
160	0.0492	0.0154	0.000	0.085	0.046	0.249	0.443	0.563	0.176
161	0.0890	0.0000	0.000	0.039	0.000	0.000	0.961	0.985	0.000
162	0.0888	0.0000	0.000	0.000	0.000	0.000	1.000	1.000	0.000

APPENDIX C

SAMPLE CALCULATION AND MASS BALANCE

The experimental data for this calculation pertains to Run No. 193.

A. Sample Calculation

1. Reactants and other parameters

$$P_f = \frac{7.36 \text{cu.cm./hr} \times 0.983 \text{gm/cu.cm.}}{79.1 \text{gm/gmole}}$$

$$= 0.0915 \text{ gmoles/hour}$$

$$\text{moles } H_2\text{/hour} = \frac{1396 \text{cu.cm./min} \times 60 \text{min/hr.}}{22400 \text{gmole/cu.cm.}}$$

$$= 3.7393 \text{ gmoles/hour}$$

$$\text{mole fraction pyridine} = \frac{0.0915}{(0.0915+3.7393)}$$

$$= 0.02388$$

$$P_{p_o} = 5.617 \text{ M Pa} \times 0.02388 = 0.1341 \text{ M Pa}$$

$$= 134.1 \text{ k Pa}$$

$$W = \frac{10.365 \text{ gm}}{0.792 \text{ gm/cu.cm.}} = 13.087 \text{ cu.cm.}$$

$$F = 0.0915 \text{ gmole/hr} \times 22400 \text{ cu.cm-atm/gmole} \times \frac{1.0133 \times 10^5 \text{ Pa/atm}}{5.617 \times 10^6 \text{ Pa}}$$

$$= 36.97 \text{ cu.cm./hr.}$$

$$t = W/F = \frac{13.087 \text{ cu.cm.}}{36.97 \text{ cu.cm./hr.}}$$

$$= 0.3541 \text{ hr.}$$

2. Analysis with reactor bypassed

Area of pyridine peak = 655.0 area units.

$$\text{Pyridine quantity in sample} = \frac{655.0 \text{ area units} \times 0.78 \text{ mass unit/area unit}}{79 \text{ gm/gmole}}$$

$$= 6.4649 \text{ gmole/mass unit}$$

But this corresponds to a molal flow rate of 0.0915 gmoles/hr.

Thus, a proportionality constant Q can be calculated as:

$$Q = \frac{0.0915 \text{ gmole/hr}}{6.4649 \text{ gmole/mass unit}}$$

$$= 1.4153 \times 10^{-2} \text{ mass unit/hr.}$$

This constant Q is a function of sample size only.

3. Analysis with reactor in line

Area of pyridine peak = 322.14 units.

Area of piperidine peak = 320.77 units.

Pyridine quantity in sample

$$= \frac{322.14 \text{ area units} \times 0.78 \text{ mass units/area unit}}{79 \text{ gm/gmole}}$$

$$= 3.1795 \text{ gmole/mass unit}$$

Pyridine flow rate

$$= 3.1795 \text{ gmole/mass unit} \times 1.4153 \times 10^{-2} \text{ mass unit/hr}$$

$$= 0.0450 \text{ gmole/hr.}$$

Piperidine quantity in sample

$$= \frac{320.77 \text{ area units} \times 0.83 \text{ mass units/area unit}}{85 \text{ gm/gmole}}$$

$$= 3.1307 \text{ gmole/mass unit}$$

Piperidine flow rate

$= 3.1307$ gmole/mass unit $\times 1.4153 \times 10^{-2}$ mass unit/hr.

$= 0.0443$ gmole/hr.

Moles piperidine formed per mole pyridine feed

$$= \frac{0.0443 \text{ gmoles/hr}}{0.0915 \text{ gmoles/hr}}$$

$= 0.4842$

Moles unreacted pyridine per mole of pyridine feed

$$= \frac{0.0450 \text{ gmole/hr}}{0.0915 \text{ gmole/hr}}$$

$= 0.4918$

Normalized piperidine mole-fraction in products

$$= \frac{0.4842}{0.4842+0.4918}$$

$= 0.496$

Normalized pyridine mole-fraction in products

$$= \frac{0.4918}{0.4812+0.4918}$$

$= 0.504$

Fractional conversion, $x = 0.496$.

B. Mass Balance

The stoichiometric equation for the reaction is:

$$\text{Pyridine} + 3H_2 \longrightarrow \text{Piperidine}$$

Hydrogen has not been analyzed for and as such does not appear in the mass balance.

Basis: One hour

Input: C in feed

= 0.0915 gmole x 5 gm.atom/gmole

= 0.4575 gm atoms

N in feed

= 0.0915 gmole x 1 gm.atom/gmole

= 0.0915 gm atoms

Output: C in piperidine

= 0.0443 gmole x 5 gm.atom/gmole

= 0.2215 gm atoms

C in unreacted pyridine

= 0.0450 gmole x 5 gm atom/gmole

= 0.2250 gm atoms

Total C out = 0.2215 + 0.2250

= 0.4465 gm atoms

N in piperidine = 0.0443 gmole x 1 gm atom/gmole

= 0.0443 gm atoms

N in unreacted pyridine

= 0.0450 gmole x 1 gm atom/gmole

= 0.0450 gm atoms

Total N out = 0.0893 gm atoms.

Percent deviation in C balance

$$= \left(\frac{0.4575-0.4465}{0.4575}\right) \times 100\%$$

= 2.40%

Percent deviation in N balance

$$= \left(\frac{0.0915-0.0893}{0.0915}\right) \times 100\% = 2.40\%$$

APPENDIX D

EXTERNAL TRANSPORT

The temperature and partial pressures of different substances at the catalyst have been calculated for a typical run by the method of Yoshida et al[29]. The data is taken from Run. No. 174.

Temperature: 145°C

W/F: 0.3541 hours

P_{p_o}: 106.0 k Pa

W: 10.365 grams

COMPOUND	FEED RATE MOLES/HOUR	PRODUCT RATE MOLES/HOUR
Pyridine	0.0915	0.0489
Piperidine	0.0000	0.0415

A. Estimation of Partial Pressure

Partial pressure drops were calculated from Yoshida, Ramaswami, and Hougen's plot[29]. The following parameters have been defined:

$$R' = \frac{r_j}{a_m \phi G_m}$$

where R' is a dimensionless parameter,

r_j is molal reaction rate of component j per unit mass of catalyst,

a_m is surface area of catalyst, sq.cm./gm.,

ϕ is shape factor (0.90 for irregular shapes),

G_m is molal mass velocity of gas based on total cross-section of the bed.

Hence,

$$r_{pyr} = r_{pip} = \frac{0.0915-0.0489}{10.365}$$

$$= 4.1100 \times 10^{-3} \text{ gmoles/hr-gm. catalyst}$$

$$a_m = 203 \text{ sq.m/gm.}$$

$$= 2.03 \times 10^{6} \text{ sq.cm./gm.}$$

$$G_m = \frac{0.0915 \times 5.62}{0.106 \times (\frac{1.05^2}{4})}$$

$$= 5.6025 \text{ gmoles/hr-sq.cm.}$$

$$R' = \frac{4.1100 \times 10^{-3}}{2.03 \times 10^{6} \times 0.9 \times 5.6025}$$

$$= 4.0153 \times 10^{-10}$$

$$y_{pyr} = (y_{j_{in}} + y_{j_{out}})/2$$

$$y_{pyr} = \frac{(0.0915+0.0489) \times 0.106}{2 \times 5.62}$$

$$= 1.3241 \times 10^{-3}$$

$$y_{pip} = \frac{(0+0.0415) \times 0.106}{2 \times 5.62}$$

$$= 3.9137 \times 10^{-4}$$

Then,

$$(\frac{R}{y})_{pyr} = \frac{4.0153 \times 10^{-10}}{1.3241 \times 10^{-3}}$$

$$= 3.0325 \times 10^{-7}$$

$$\left(\frac{R}{y}\right)_{pip} = \frac{4.0153 \times 10^{-10}}{3.9137 \times 10^{-4}}$$

$$= 1.0260 \times 10^{-6}$$

From the plot,

$$\text{maximum } \left(\frac{\Delta P}{P_t}\right)_{pyr} < 10^{-6}$$

$$\text{maximum } \left(\frac{\Delta P}{P_t}\right)_{pip} < 10^{-5}$$

The partial pressures at the catalyst surface are thus found to be very close to those in the bulk gas phase.

B. Estimation of Temperature at Catalyst Surface

The temperature at the catalyst surface has also been estimated by the method of Yoshida et al[29].

A parameter Q_p is defined as:

$$Q_p = \frac{r_j \Delta H_R}{a_m \phi C_p G_m}$$

where C_p is the molal heat capacity

and ΔH_R is the heat of reaction.

Now, ΔH_R = 373 k cal/gmole

C_p = 20 cal/gmole-°K

So,

$$Q_p = \frac{4.1100 \times 10^{-3} \times 373000}{2.03 \times 10^{6} \times 0.9 \times 20 \times 5.6025}$$

$$= 7.49 \times 10^{-6}$$

Then, from the plot[29],

$$\Delta T = 10^{-5}\ ^{\circ}C \text{ (max.)}$$

Thus, the temperature at the catalyst surface was equal to the bulk stream temperature.

APPENDIX E

INTERNAL TRANSPORT

The extent of transport processes in the interior of the catalyst was evaluated to see if diffusion was rate-controlling.

A. Molecular Diffusion

The extent of molecular diffusion was estimated by varying the flow rate of reactants across the reactor bed at a constant pressure temperature, initial pyridine partial pressure and residence time. The variation in conversion obtained is an indication of the extent of molecular diffusion.

P_{po}: 106.0 k Pa

Temperature: 130°C

Total Pressure: 5.617 M Pa

Residence Time: 0.1755 hours

RUN NO.	CAT. gms.	p_f	PRODUCT RATE		PRODUCT COMPOSITION		CONVERSION %
			Pyr.	Pip.	Pyr.	Pip.	
231	2.750	0.0490	0.0374	0.0112	0.770	0.230	23.0
232	4.050	0.0721	0.0564	0.0177	0.761	0.239	23.9
233	5.140	0.0915	0.0732	0.0220	0.769	0.231	23.1
234	7.830	0.1394	0.1031	0.0329	0.758	0.242	24.2
176	10.365	0.1845	0.1395	0.0431	0.764	0.236	23.6

The variation in the conversion with flow rate is within the limits of experimental error and as such it was concluded that molecular diffusion was not controlling.

B. Pore Diffusion

The extent of pore diffusion was determined by measuring the conversion at conditions identical to those in one of the experimental runs but with a smaller catalyst particle size.

Pressure: 5.62 M Pa

Temperature: 145°C

p_f: 0.1845 g moles/hr.

P_{p_o}: 106.0 k Pa

Catalyst Quantity: 10.365 gms.

RUN NO.	CATALYST SIZE		PRODUCT RATE		PRODUCT COMPOSITION		CONVERSION %
	MESH	$D_{P,MM}$	Pyr.	Pip.	Pyr.	Pip.	
235	-40,+60	0.335	0.1380	0.0418	0.768	0.232	23.2
176	-20,+40	0.630	0.1395	0.0431	0.764	0.236	23.6

If pore diffusion was of significance, a reduction of the particle size should have resulted in enhanced conversion. As this was not found to be the case, it was concluded that pore diffusion was negligible.

APPENDIX F

LEAST SQUARES FITTING

CONSTANTS CALCULATED BY LEAST SQUARES FITTING

CALCULATION OF THE ORDER OF THE REACTION IN PYRIDINE

TEMPERATURE = 115 DEGREES CELSIUS

REACTION RATE CONSTANT = 2.698
ORDER OF THE REACTION IN PYRIDINE = 2.23

COMPARISON OF CALCULATED AND EXPERIMENTAL RESULTS

LN PPO	LN RATE(EXP)	LN RATE(CALC)	ERROR%
-3.0642	-4.0906	-4.1331	1.0378
-2.8292	-3.6848	-3.6092	2.0525
-2.5279	-2.9043	-2.9375	1.1426

TEMPERATURE = 130 DEGREES CELSIUS

REACTION RATE CONSTANT = 3.116
ORDER OF THE REACTION IN PYRIDINE = 2.15

COMPARISON OF CALCULATED AND EXPERIMENTAL RESULTS

LN PPO	LN RATE(EXP)	LN RATE(CALC)	ERROR%
-3.0642	-3.4208	-3.4593	1.1257
-2.8292	-3.0236	-2.9550	2.2680
-2.5279	-2.2784	-2.3085	1.3197

TEMPERATURE = 145 DEGREES CELSIUS

REACTION RATE CONSTANT = 1.789
ORDER OF THE REACTION IN PYRIDINE = 1.50

COMPARISON OF CALCULATED AND EXPERIMENTAL RESULTS

LN PPO	LN RATE(EXP)	LN RATE(CALC)	ERROR%
-3.0642	-2.8147	-2.8162	0.0534
-2.8292	-2.4657	-2.4630	0.1076
-2.5279	-2.0091	-2.0103	0.0574

TEMPERATURE = 160 DEGREES CELSIUS

REACTION RATE CONSTANT = 1.647
ORDER OF THE REACTION IN PYRIDINE = 1.30

COMPARISON OF CALCULATED AND EXPERIMENTAL RESULTS

LN PPO	LN RATE(EXP)	LN RATE(CALC)	ERROR%
-3.0642	-2.3382	-2.3329	0.2277
-2.8292	-2.0182	-2.0277	0.4692
-2.5279	-1.6405	-1.6364	0.2525

CONSTANTS CALCULATED BY LEAST SQUARES FITTING

CALCULATION OF PRE-EXPONENTIAL FACTOR AND ACTIVATION ENERGY

SECOND ORDER PSEUDO RATE CONSTANTS

PRE-EXPONENTIAL FACTOR = 17.025
EXPONENTIAL FACTOR = -5794.9

COMPARISON OF CALCULATED AND EXPERIMENTAL RESULTS

1/TEMP	LN KP(EXP)	LN KP(CAL)	ERROR%
0.002576	2.0378	2.0957	2.8403
0.002576	1.9735	2.0957	6.1903
0.002576	2.1514	2.0957	2.5918
0.002480	2.7075	2.6511	2.0824
0.002480	2.6347	2.6511	0.6219
0.002480	2.7773	2.6511	4.5435
0.002391	3.3136	3.1667	4.4330
0.002391	3.1926	3.1667	0.8116
0.002391	3.0467	3.1667	3.9405
0.002309	3.7901	3.6466	3.7866
0.002309	3.6401	3.6466	0.1789
0.002309	3.4152	3.6466	6.7763